FINAL REPORT

SELF-STRESSED SANDWICH BRIDGE DECKS

by

William Zuk
Consultant to the Virginia Highway Research Council

and

Raghupati S. Sinha
Graduate Assistant

(The opinions, findings, and conclusions expressed in this report are those of the authors and not necessarily those of the sponsoring agencies.)

Virginia Highway Research Council
(A Cooperative Organization Sponsored Jointly by the Virginia Department of Highways and the University of Virginia)

In Cooperation with the U. S. Department of Transportation
Federal Highway Administration

Charlottesville, Virginia

November 1971
VHRC 71-R12

ABSTRACT

Proposed is an entirely new type of bridge deck, consisting of an unreinforced lightweight concrete slab made of expanding cement sandwiched between two thin plates of steel. The expanding core serves to prestress the panel. Laboratory tests were conducted on the expansion characteristics of the concrete to determine predictable relationships for expansion. Laboratory tests were also conducted on ten small-scale panels, some loaded with a concentrated load and others with a uniformly distributed load. Instrumentation was installed to measure strains and deflections.

Mathematical theories were also developed to predict both the prestressing and external load behavior of the panels. A satisfactory correlation was found between the test results and the theory. A comparative study of the proposed sandwich panels and standard reinforced concrete slabs indicated that the proposed sandwich panels are substantially stronger and stiffer than concrete slabs using the same quantity of concrete and steel.

Continued development is recommended.

FINAL REPORT

SELF-STRESSED SANDWICH BRIDGE DECKS

by

William Zuk
Consultant to the Virginia Highway Research Council

and

Raghupati S. Sinha
Graduate Assistant

INTRODUCTION

The evolution of this research program is outlined in the series of six working plans and progress reports dating from March 1968, and listed in detail in the subsummation of the cover letter to this report. In brief, the project was started with the fabrication of a few pilot test beams and columns in a new way using thin steel plates attached to the top and bottom sides of an unreinforced lightweight concrete core made with an expanding cement. Steel studs, extending through the core and welded to the face plates, were used to bind the composite structure together. The expanding concrete further served to prestress the structure.

Results of the pilot tests proved so promising that the project was extended to study panels in which steel plates were attached to all sides of the core as shown in Figure 1. Such sandwich panels were envisioned as a possible new type of bridge deck possessing a high strength to weight ratio and permitting longer than usual bridge spans with less dead weight. In addition, such decks could be factory prefabricated, thus eliminating the many problems of constructing cast-in-place concrete decks. As will be shown, the results of this study justified these expectations.

Throughout, the work "plate" refers only to the face plate; and the word "panel" refers to the composite sandwich panel consisting of the face plates and core.

060657

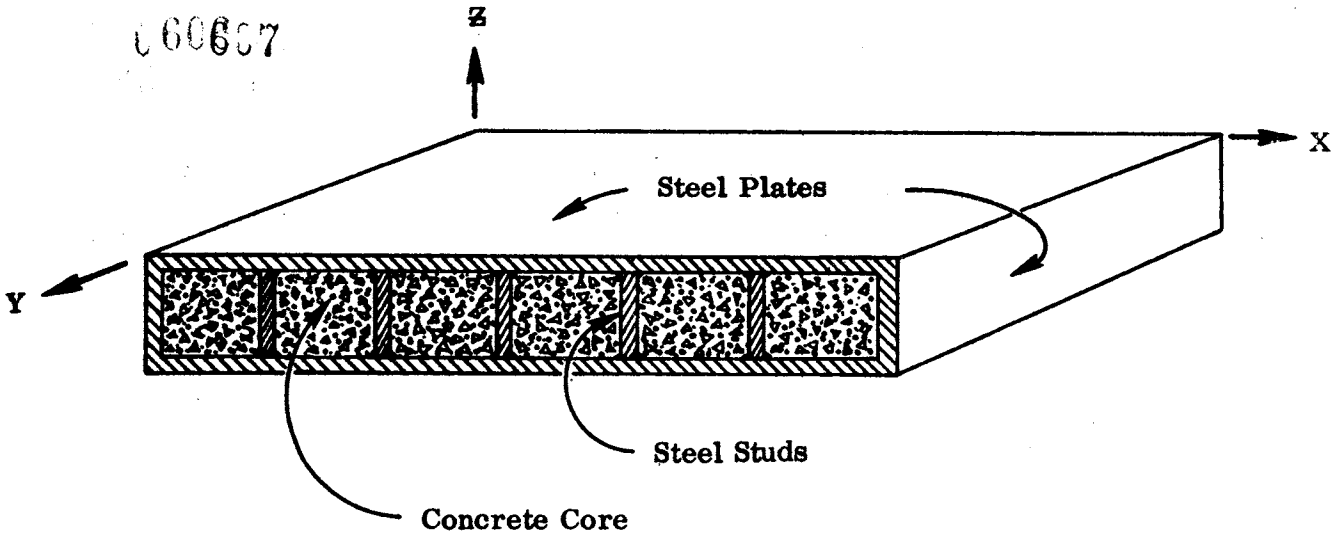

Figure 1. Section of sandwich panel.

FABRICATION OF PANELS

As the proposed sandwich panel is a type entirely new to the construction industry, a feasibility study was undertaken to assess the practicality of different methods of fabricating it. Automated and machine processes were given priority as only by such methods can fabricating costs be minimized. From this assessment, it is believed that for quantity production of the proposed sandwich panels the following procedure is feasible. (Deck panels approximately 8 feet by 10 feet by 4 inches thick with $\frac{1}{4}$ inch thick steel face plates and $\frac{3}{8}$ inch diameter steel studs 12 inches on center are visualized.) After all plates and studs are cut to size, the bottom plate is laid in a horizontal position. The four side plates are clamped and welded to the bottom plate by an automatic welder. The studs are then welded to the bottom plate in the fashion of an automatic Nelson stud welder. The top plate is placed with the positions of the studs premarked on the top surface, and is welded to the side plates in a normal fashion. To weld the top of the studs to the plate, high amperage arc welders are available which can simultaneously burn through the top plate (from above) at the positions of the studs and puddle a weld between the top of the stud and the burned hole in the plate. This procedure allows all work to be done from the accessible top surface.

An alternate procedure for welding the studs to the top plate is to prepunch small holes in the positions of the studs and use normal plug welding.

As is true in the welding of any unstiffened thin plate, care must be exercised to prevent the heat from causing large buckling or warping distortions.

The lightweight concrete core material can be pumped into the panel at the fabricating plant or at the bridge site. For control purposes it is better to place the concrete at the plant; however, this does add to the shipping weight. The concrete is pumped through small holes (approximately 4 inches in diameter) in the top plate. Additionally, several small bleeder holes in the top plate will ensure that all cavities are filled. A vibrator placed on the steel shell will further aid consolidation. After the panel is filled, the access and bleeder holes can be sealed by welding steel cover plates flush with the face plate. The concrete subsequently hardens and expands autogeneously inside the steel shell to form an extremely strong composite self-stressed sandwich panel.

When the panels are used for bridge decks, a skid resistant surfacing must be applied, either in the plant or in the field. A protective coating must also be applied to the exterior of the panel, probably in the form of paint; although the use of a weathering steel such as Cor-ten or Mayari-R might be used to preclude the need for painting. However, both alternatives have been extensively studied in connection with orthotropic steel bridge decks and the problems they present are thus not unique to the sandwich panels under consideration.

The ten test panels used in this study, however, were fabricated by manual methods, as automation was not economically warranted. The plate dimensions are given in Table 1. It is to be noted that the plan size of the plate is limited by the throat dimensions of the Universal testing machine available to conduct the loading tests. In all cases, the plate was simply supported on all four sides and had an effective span of 23.5 inches.

TABLE I

PLATE DIMENSIONS

Panel No.	Thickness in inches			Stud			Plan Size in in.
	Face	Core	Total	Dia. (in.)	Tot. No.	Pattern*	
P_1	.140	2.51	2.79	.25	36	(a)	25 x 25
P_2	.076	1.348	1.50	.25	36	(a)	25 x 25
P_3	.075	1.038	1.19	.125	36	(a)	25 x 25
P_4	.076	1.118	1.27	.25	1	(f)	25 x 25
P_5	.076	1.120	1.27	.25	10	(d)	25 x 25
P_6	.074	1.032	1.18	.25	4	(e)	25 x 25
P_7	.076	1.078	1.23	.25	33	(b)	25 x 25
P_8	.075	1	1.15	.25	36	(a)	27 x 27
P_9	.075	1	1.15	.25	16	(c)	27 x 27
P_{10}	.075	1	1.15	—	none	—	27 x 27

*See Figure 2.

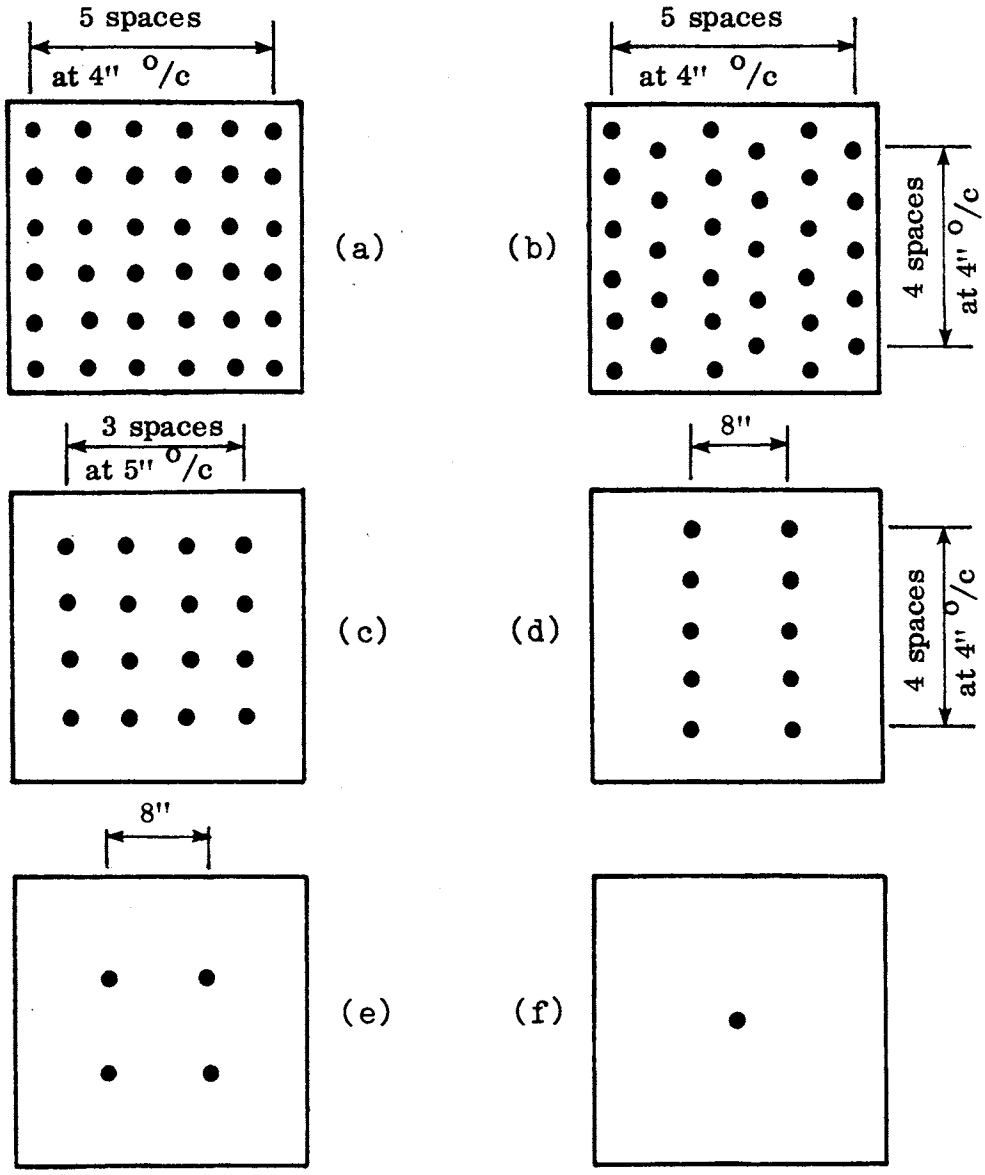

Figure 2. Stud patterns.

Seven panels, P_1 through P_7, were fabricated as shown in Figure 3, with the top of the studs protruding through predrilled holes in the top plate. This arrangement permitted the use of simple fillet welds throughout the panel. As a certain amount of plate warping was caused by the heat of welding, it was decided to try an all cold bolted fabrication method, shown in Figure 4, for the last three panels, P_8 through P_{10}. Bolting eliminated the warping problem, and worked well for the experiments; however, it required more manual operations for assembly, and thus would not be very desirable for any type of plant production. (The added dimension of the tube edging resulted in these panels being two inches bigger than the welded panels, although the effective support length was unchanged.)

The steel for the face plates and studs conformed to ASTM A-7 and ASTM G-5 specifications, respectively.

The concrete core material was placed by hand in either a side or top opening while the panel was being vibrated on a shake table to ensure proper filling. The openings were then sealed. The proper type and mix proportions of the concrete was arrived at only after considerable pretesting, which is described in the next section. However, to summarize, the mix finally used consisted of coarse aggregate of expanded shale (with a maximum size of $\frac{1}{2}$" and a fineness modulus of 7.565), class A silica sand, type K expansive cement (furnished by the Southwestern Portland Cement Company and called Chem-Stress), and water. The mix by weight was 1 part cement, 0.5 part sand, 1 part coarse aggregate and 0.34 part free water. (The coarse aggregate was presoaked 48 hours for internal saturation.) The slump averaged 5 inches and the unit weight was 122 pounds per cubic foot. The average 28-day compressive strength was 1738 psi.

As the panels were all moisture sealed, the concrete hardened autogeneously with no addition or subtraction of water at room temperature.

Panels P_1 through P_7 were allowed to cure for 28 days prior to testing; whereas (because of scheduling problems) panels P_8 through P_{10} cured for only 14 days.

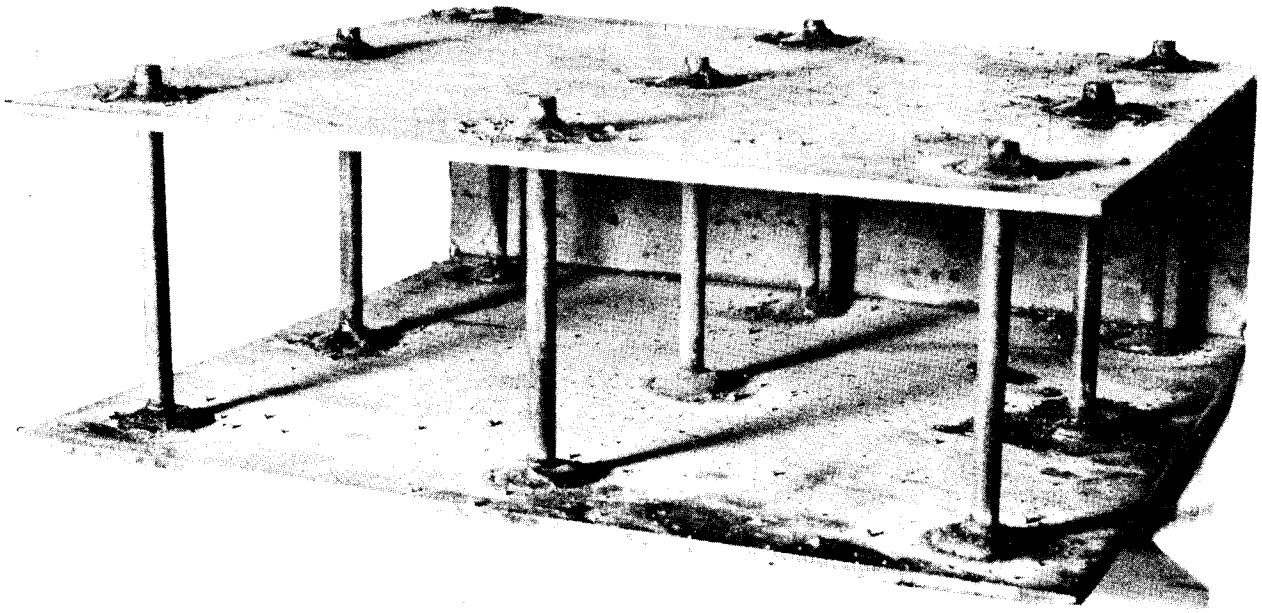

Figure 3. Welded panel assembly.

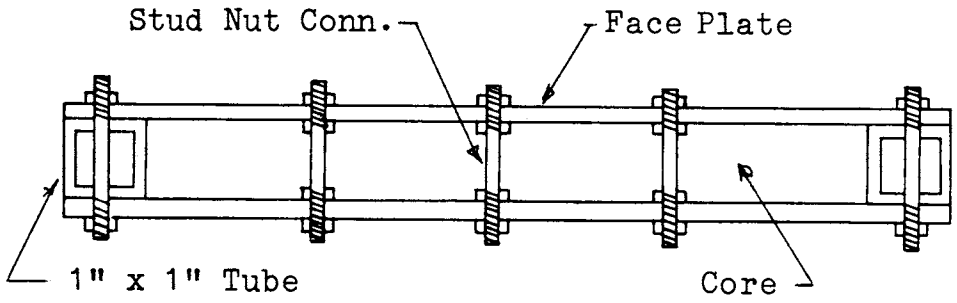

Figure 4. Bolted test panel construction.

PROPERTIES OF CORE MATERIALS

Contained in reference (1), prepared by ACI Committee 223, is a recent list of 62 papers relating to the present knowledge of expansive cement concrete. Although a number of these references bear obliquely on the core material as used in the sandwich panels in this study, in total the known data on the subject were insufficient to afford a proper understanding of the behavior of expanding lightweight concrete in a moisture sealed, expansion restraining panel. Thus, it was necessary to conduct a series of tests to ascertain the properties of the core material, particularly under different conditions of restraint. In all, 170 specimens were cast using 10 different mixes of concrete and 7 different percentages of steel reinforcing, which functioned as elastic restraints. It is necessary to understand the nature of the core material under elastic restraint because the expanding concrete in the core of the panel is subject to the restraint of the steel shell. By increasing the thickness of the steel face plates, the percent of steel (based on the gross cross sectional area of the panel) is increased; restraint is increased and the expansion is thereby decreased.

Tables 2 and 3 describe the properties of the 10 batches of concrete tested; batches 1 - 5 used shrinkage-compensating cement and batches 6 - 10 used self-stressing cement. Tests of the two types of cement will be described separately.

The 5 different mixes of shrinkage-compensating cement concrete were tested with the percentages of reinforcing steel being varied from 2.78 to 16.69 percent. Unrestrained specimens were also made for comparison. The cement was a commercially available "Chem-comp" shrinkage-compensating type. The coarse aggregate was expanded shale with a maximum size of $\frac{1}{2}$ inch and a fineness modulus of 7.565. This lightweight aggregate was presoaked 48 hours for saturation. The sand was class A silica sand. The steel was intermediate grade deformed reinforcing bars. The specimens were molded in standard 6-inch diameter by 12-inch long cylinders, in which brass plugs were inserted 10 inches apart for the purpose of taking expansion readings by a Whittemore strain gage. The reinforcing bars were placed uniaxially in the long direction of the cylinder. Duplicate specimens were made of all castings, except for the standard 6 inch by 12 inch unreinforced cylinders cast for obtaining 28-day strengths, which were cast in triplicate. Thus 85 specimens were cast.

Six hours after casting, the forms were stripped, initial gage point readings were taken and the specimens' moisture sealed in double polyethylene bags. Storage was at room temperature. Expansion readings were taken periodically for the next 28 days.

Figure 5 shows the readings at the 28th day (at which time the expansion was essentially stable) for the 5 types of concrete and the various percentages of reinforcing. It may be observed that there is a certain amount of scatter in these data at the scale shown. As previously reported by other investigators in reference (1), expansion is very sensitive to a number of factors such as water-cement ratio, curing, temperature, size of specimen, mixing time, admixtures, aggregate types, and age of the cement. A combination of these factors, coupled with normal experimental errors, could account for the scatter at this small scale of expansion. However, the trend toward less expansion is evident as the percentage of reinforcing or restraint is increased.

TABLE 2

PROPERTIES OF SHRINKAGE COMPENSATING CONCRETES

Properties	Batch 1	2	3	4	5
Mix proportion (by wt.)					
Water	0.40	0.38	0.40	0.45	0.35
Cement	1.00	1.00	1.00	1.00	1.00
Sand	1.25	1.10	1.20	1.20	0.67
Coarse agg.	0.87	0.93	0.90	1.14	0.87
Water (pcf)	126	115	120	119	108
(kg/m^3)	2018	1842	1922	1906	1730
28-day Compr. str. (psi)	4786	3866	3883	4432	3477
(kgf/cm^2)	337	272	273	312	244

TABLE 3

PROPERTIES OF SELF-STRESSING CONCRETES

Properties	6	7	8	9	10
Mix proportion (by wt.)					
Water	0.34	0.34	0.42	0.50	0.39
Cement	1.00	1.00	1.00	1.00	1.50
Sand	0.50	0.75	0.75	0.75	0.75
Coarse agg.	1.00	1.00	1.50	1.50	1.50
Weight (pcf)	122	122	114	114	117
(kg/m^3)	1954	1954	1826	1826	1874
*28-day Compr. str. (psi)	1738	1950	2055	1840	1561
(kgf/cm^2)	122	137	145	129	110

*These values are based on unreinforced concrete which develops weakening micro-cracks. The same concrete reinforced, which inhibits such cracks, would produce strengths approximately $2\frac{1}{2}$ times higher.

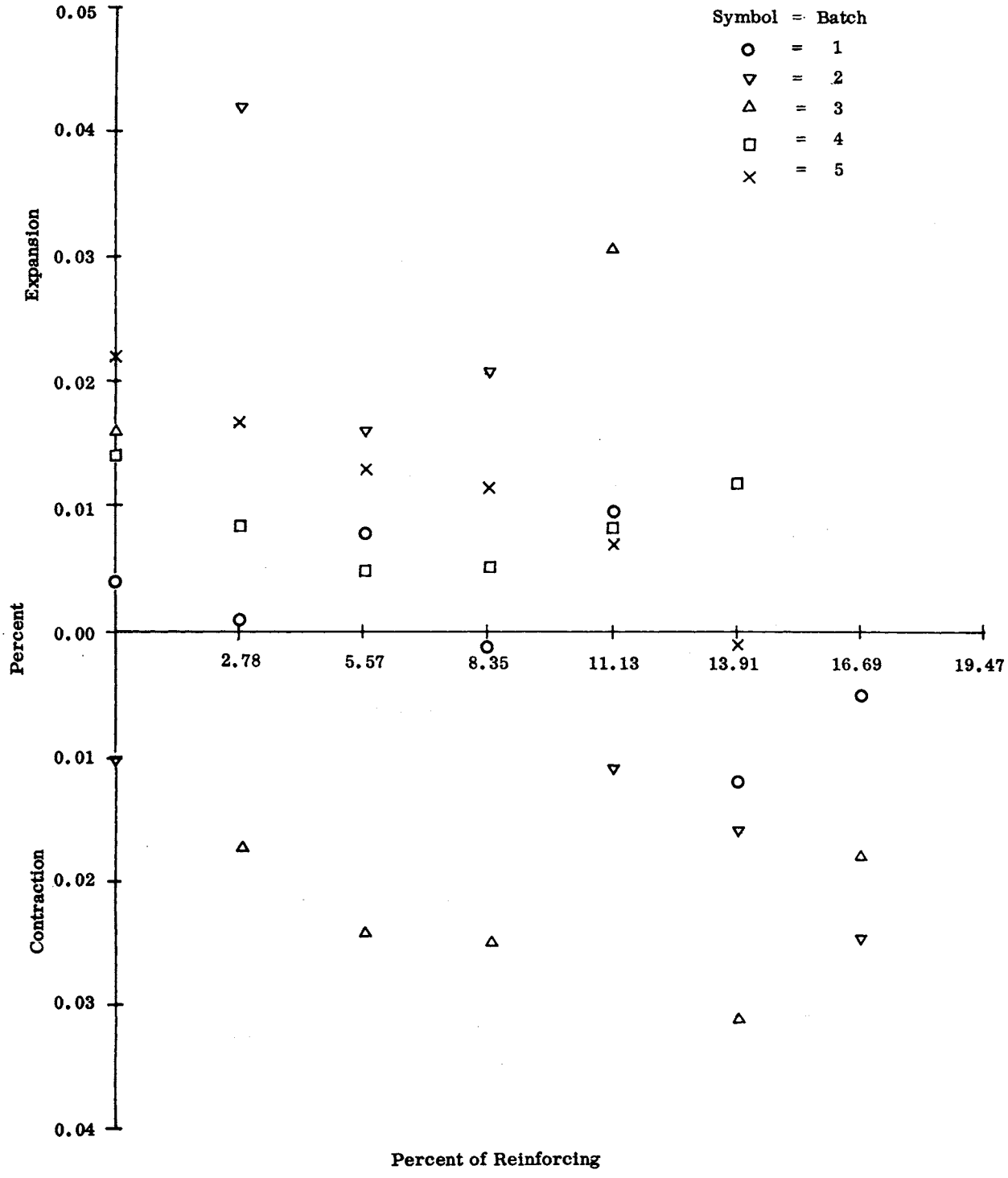

Figure 5. Expansion of shrinkage-compensating concrete at 28 days.

Indeed, at high degrees of restraint, there is a net contraction or shrinkage. This unexpected phenomenon can be explained by observing Figure 6, the general expansion behavior observed on unreinforced specimens as a function of time under autogenous curing. Note that there is first an expansion phase, followed by a contraction phase, followed by a lesser expansion phase. For lightly restrained conditions, the amount of movement is of the same nature, but less than for free expansion. However, for heavily restrained conditions, the initial expansion phase is essentially inhibited. Thus, in the contraction phase, a net shrinkage is induced. The result is a small contraction at the end of 28 days. Based on these data, the optimum amount of reinforcing to minimize net long-term movement in such concretes is on the order of 12%, although amounts as low as 5% appear to be practically as effective.

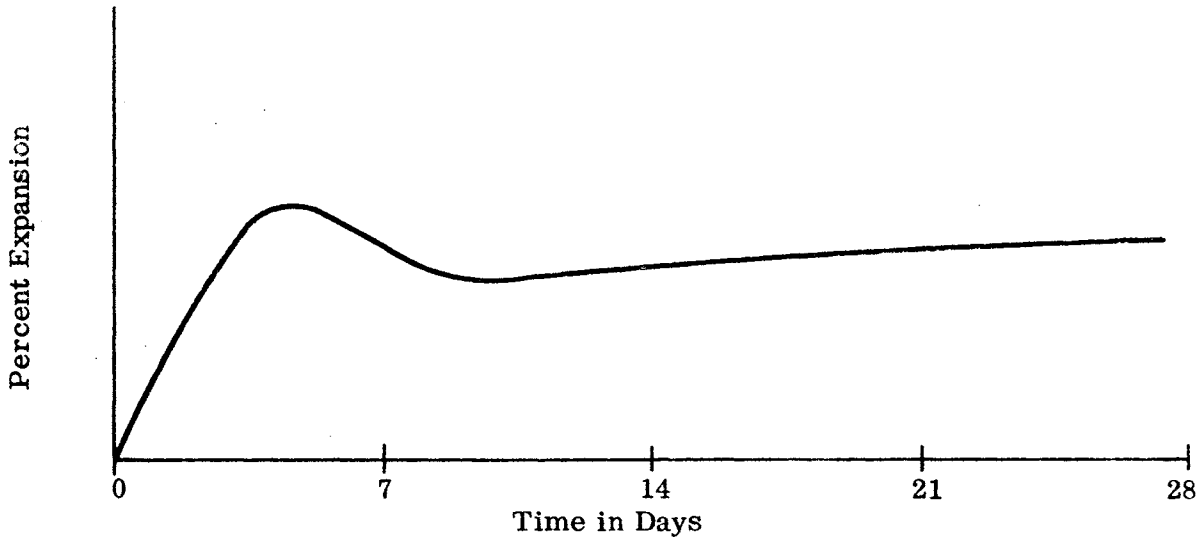

Figure 6. Typical reinforced time-expansion behavior for shrinkage compensating cement concrete (non quantitative).

For tests with self-stressing cement concrete, the percentage of steel reinforcing used ranged from 2.16 to 13.7, represented by bars of 1/2, 3/4, 7/8, 1, 1-1/8, and 1-1/4 inches in diameter. The expansive cement used was type K obtained from the Southwestern Portland Cement Company. The same lightweight aggregate (expanded shale) and sand was used as in the previously described tests with shrinkage-compensating cement. The reinforcing was again of intermediate grade steel. Instead of using deformed bars, a single smooth bar was used, on whose ends were welded 3 inch by 3 inch by 3/4 inch thick cap plates, as shown in Figure 7. These capped bars were placed in standard steel molds, as shown in Figure 8, such that prismatic test specimens 3 inches by 3 inches by 11 inches long (including the cap plates) could be cast. This type of specimen proved to be much easier to make than the cylindrical specimens described before, and allowed expansion readings to be taken by a 10-inch Whittemore strain gage by measuring the spread of gage points in the two opposite cap plates. It may be noted that the reinforcing bar was lightly oiled before casting to break any bond between the bar and the concrete, and thus permit the full force of the expansion to bear on the end cap plates. Sixty such specimens were cast, two each for each of five types of concrete used with each size bar. In addition 15 standard 6" dia. by 12" cylinders were cast, three for each concrete mix. These were used to observe unrestrained behavior and for strength tests. After being stripped, the specimens were placed in triple polyethylene bags for autogenous curing at a constant room temperature.

Periodically, for 8 weeks, strain readings were taken. The maximum expansion was reached in about 4 weeks, as seen in the typical expansion-time curve shown in Figure 9. Note additionally that about 90% of the full expansion is reached by the 3rd day and that there is a slight falling off of expansion after the 4th week (about 2% of full expansion).

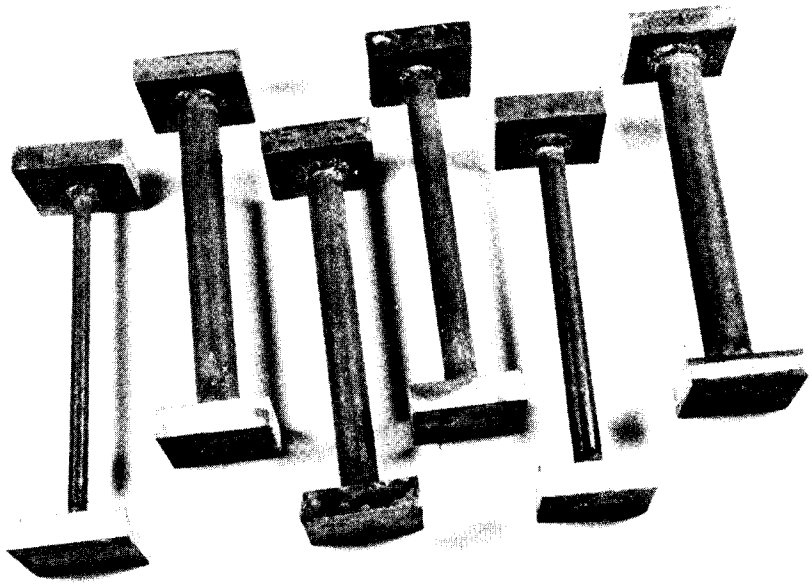

Figure 7. Reinforcing configurations.

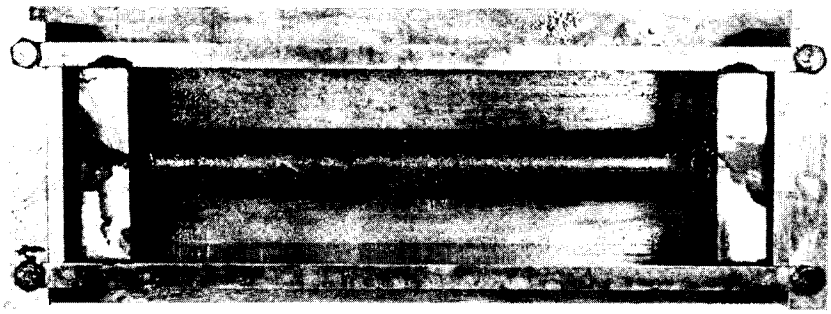

Figure 8. Specimen mold with reinforcing.

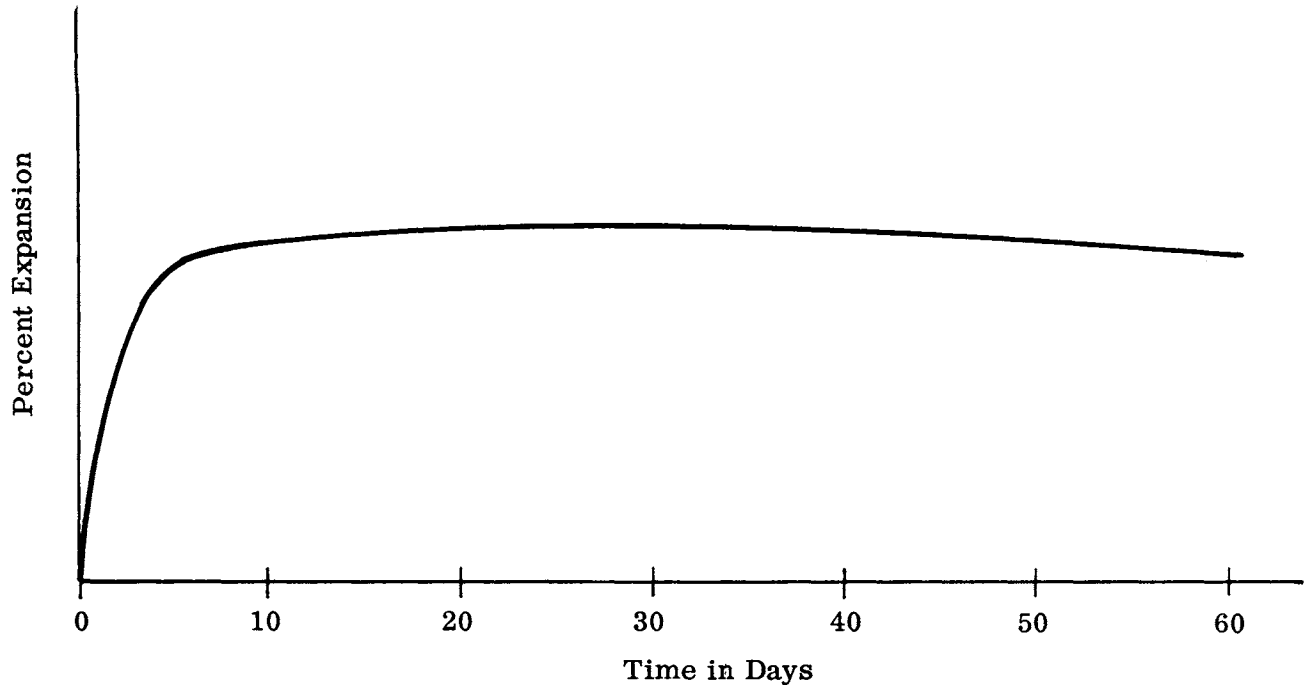

Figure 9. Typical reinforced time-expansion behavior for shrinkage compensating cement concrete (non quantitative).

Graphs of the expansion for the 5 mixes at different percentages of reinforcing at 4 weeks (28 days) are shown in Figure 10.

Equations for these curves were found with high statistical accuracy (correlation coefficients around 0.99) in the form of

$$r = K(p+q)^{-m} \qquad \text{--- Eq. (1)}$$

where, r = percent of expansion

$K = 0.012\ (w/c)^{-2.783}$

$m = 0.488\ (w/c)^{-0.609}$

$q = 0.003\ (w/c)^{-3.109}$

w/c = water-cement ratio

p = percent of steel reinforcing based on gross area.

Table 4 lists the constants K, m, and q as found for the 5 mixes of concrete used.

No visible cracking was observed on the restrained specimens; however, considerable micro-cracking (of the order of 0.0063 inch wide) was observed on the unrestrained specimens. Microscopic examination revealed the cracks to be of three types; (a) partially or completely around the lightweight aggregate; (b) within the cement-sand paste; and (c) within the shale aggregate itself. Of further interest is the fact that unrestrained specimens cured by full immersion in water also developed extensive micro-cracks by the 10th day, at the same time showing the presence of free calcite produced by the concrete. By means of this calcite, the cracks started healing themselves by the 28th day and fully healed themselves by the 40th day of continued immersion.

For the purpose of using expanding lightweight concrete as a core material in a composite steel-concrete sandwich panel, self-stressing cement was found to be preferable over shrinkage-compensating cement, as the former puts the concrete in a compressive prestressed state. Such precompression, in effect, increases the failure stress of the concrete; thereby increasing the strength of the panel. As constructed, these panels restrain the core strongly in two directions (X & Y, shown in Figure 1) and partially in the third (Z). More research is needed to determine if equation (1) is significantly modified under biaxial and triaxial restraint. Nonetheless, the uniaxial data thus far obtained are believed to be useful in the understanding of the behavior of expanding cement concrete. Whereas some scatter of data was observed with shrinkage-compensating cement concrete, less was observed with expanding cement concrete. This finding made it possible to determine a predictable equation of restrained expansion for expanding cement concrete, as given in equation (1).

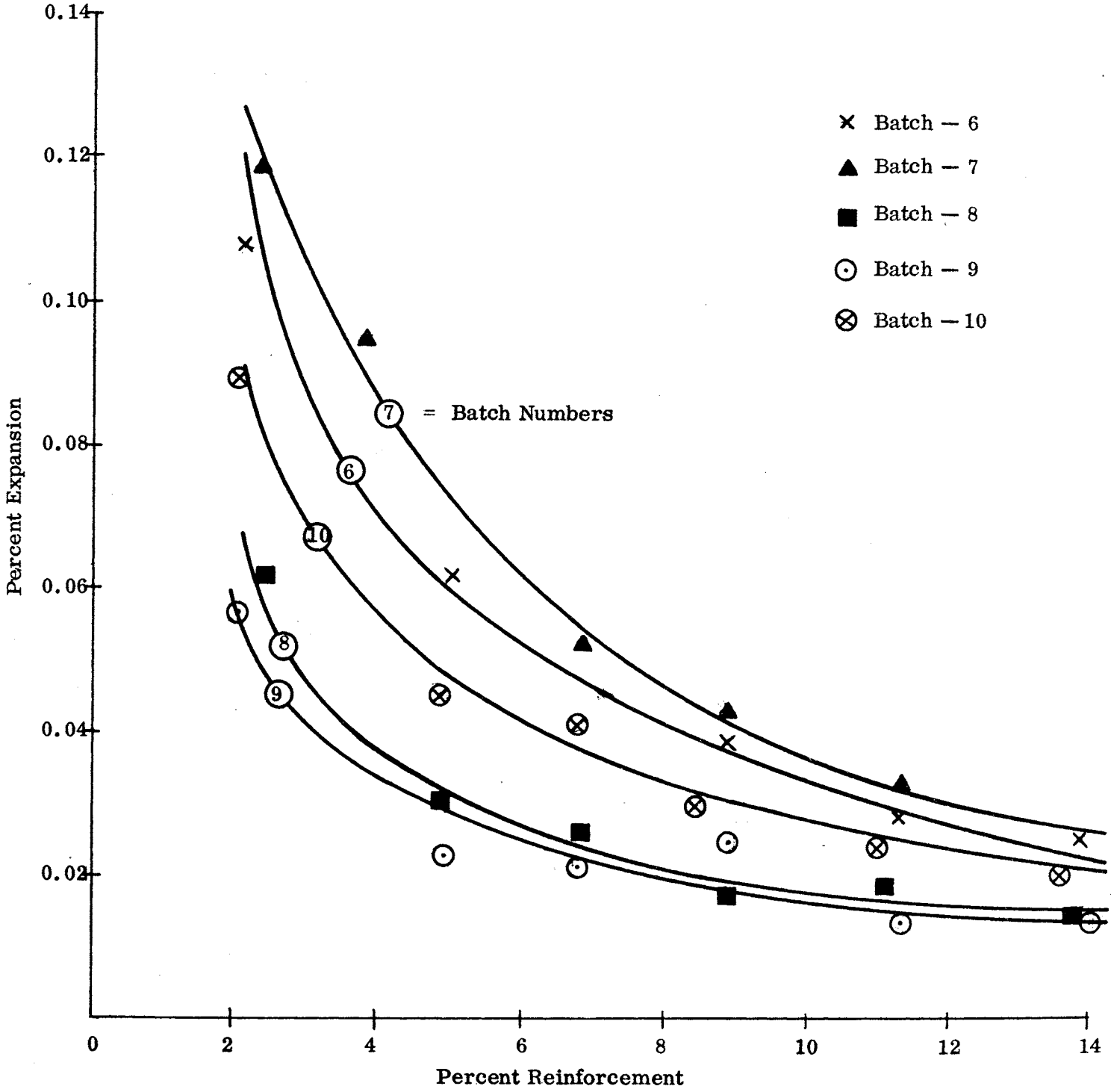

Figure 10. Expansion of self-stressing concrete.

TABLE 4

CONSTANTS FOR DETERMINATION OF EXPANSION

Constants	Batch				
	6	7	8	9	10
K	0.241	0.250	0.116	1.769	0.175
m	0.870	0.852	0.814	1.920	0.816
q	0.090	0.079	0.046	1.118	0.038

TESTING OF PANELS

Experimental testing of the panels, which was conducted in the engineering laboratory of the University of Virginia, consisted of two phases. The first involved the behavior of the prestressing action alone as the core concrete expanded, and the second involved the testing of the hardened panels with an external load. Panels $P_1 - P_7$ were loaded with a concentrated load in the center of the panel and panels $P_8 - P_{10}$ were loaded with a uniform load. All four edges were simply supported on a span of 23.5 inches by 23.5 inches in all cases.

Instrumentation to detect the behavior of the panels under prestressing forces consisted of a specially made "C" caliper (to measure changes in the thickness of the panel) and a set of electrical resistance strain gages (to measure strains in the face plates).

The thickness caliper is shown in Figure 11. The device has a clear arm length of 15 inches and is made of invar steel to minimize the effects of temperature variation. The upper arm is adjustable in the vertical, horizontal, and rotational directions for control in positioning. Mounted at the end of the upper arm is a depth micrometer, accurate to one ten-thousandth of an inch. In use, as the panel was hardening (and expanding), this caliper was slipped over the thickness of the plate at various marked positions to determine its changed thickness. However, the thickness changes during expansion were so small that the accuracy of this method of detection was insufficient. The data obtained from this test are thus not reported. Two other methods of determining movement through the thickness of the plate were also tried. One was to mount sensitive dial gages on fixed positions over the plate as it was hardening to detect relative changes in the vertical movement. This method also proved too inaccurate. A second method was to mount electrical resistance strain gages along the vertical studs inside the core. (These were placed before casting of the concrete.) Despite precautions in the waterproofing of these gages, some electrical leakage occurred and caused the gage readings to drift.

Numerous electrical resistance strain gage rosettes were also applied on the outer surface of the face plates, as shown in a typical installation in Figure 12.

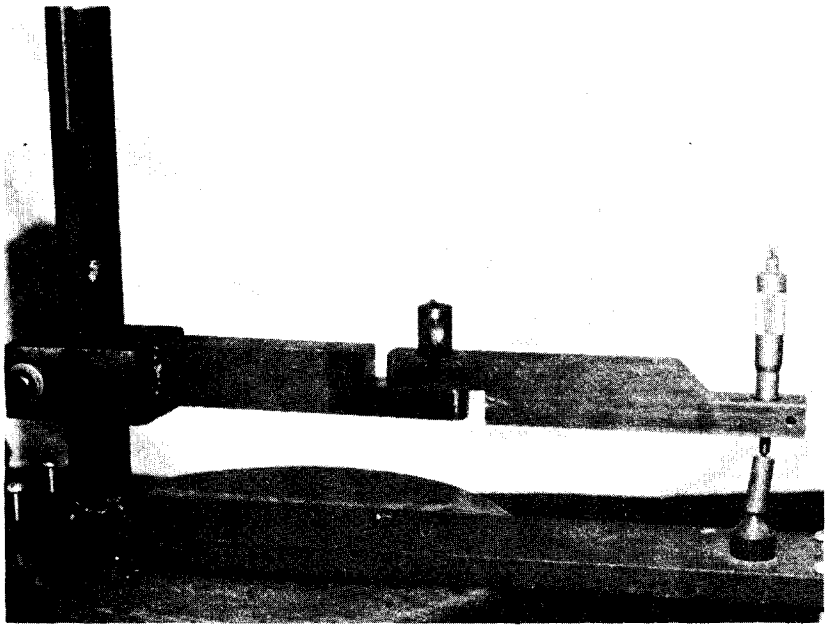

Figure 11. Thickness caliper.

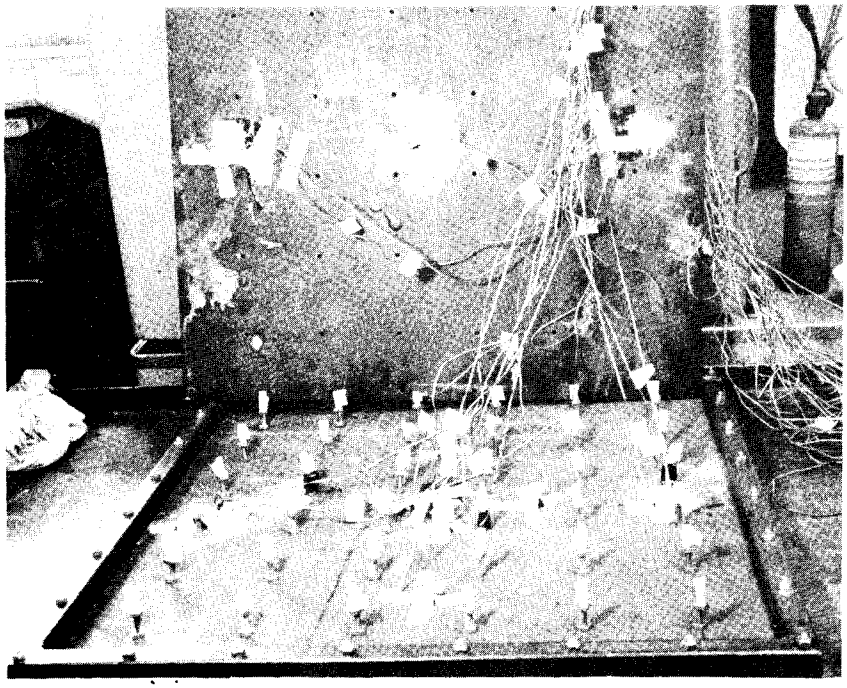

Figure 12. Typical strain gage installation.

The first seven panels fabricated were load tested using an external concentrated force at the center of the panel applied by a Baldwin Southwork Tate Energy Universal testing machine of 300,000 pound capacity. In addition to the already attached strain gages on the face plates (from the prestressing tests), six dial gages capable of reading to one ten-thousandths of an inch were mounted as shown in Figure 14 to measure the panel deflection. (Note that one gage is mounted directly over the support to detect any possible edge support deflection.)

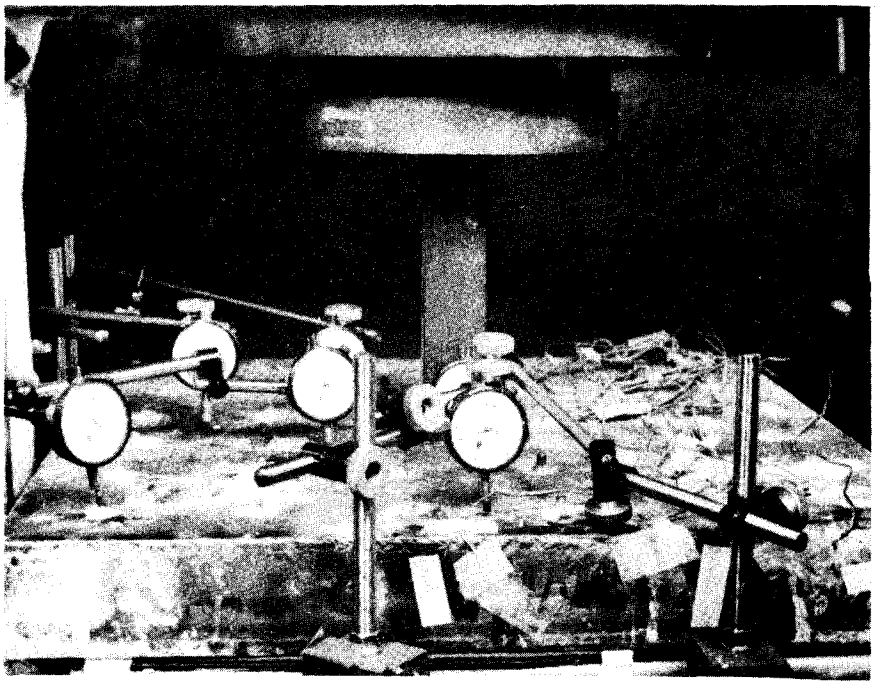

Figure 14. Application of concentrated load.

The edge supports were round bars, topped by small flat bars serving as bearing plates. Care was taken to ensure that no gaps existed between the panel and the bearing plates. The entire support system rested flat on the heavy bed of the testing machine. Despite such care in providing good support, however, deflections were noted at the edges. Unfortunately, for the purpose of the deflection data analysis, these edge deflections at the small scale of these models were of the same order of magnitude as the panel deflections (both being very small), which made it difficult to ascertain the true net deflections of the panel.

As would be normally assumed, panels with thicker cores or face plates and with more studs would be stronger (less strain per load) than panels with thinner cores or plates and less studs. Figure 15 shows this relationship through the elastic region.

The gages were attached by an epoxy adhesive (AE-10) and coated with a waterproofing compound. Switching boxes and static strain indicators were used for monitoring the strains as shown in Figure 13. The gages themselves functioned satisfactorily, however, the precise behavior of the face plates proved to be much more complex than anticipated. As will be explained more fully in the next section under the heading of Mathematical Analysis, the face plates during prestressing are simultaneously subjected to varying amounts of bending in addition to biaxial tensile stresses in the plane of the plate. The bending is caused by the expansion of the concrete perpendicular to its surface in the Z direction (see Figure 1). The face plate deflects more between the studs than at the studs, which results in variable local bending. Secondary bending also develops in the thin face plates as a result of local surface irregularities caused by fabrication errors, warping during welding, and the like. As tension is generated in the plate by virtue of the prestressing forces in the X and Y directions, these "wrinkles" tend to straighten out and cause additional bending. (It may also be mentioned that these same tensile forces affect the out of plane bending caused by the concrete swelling in the Z direction.)

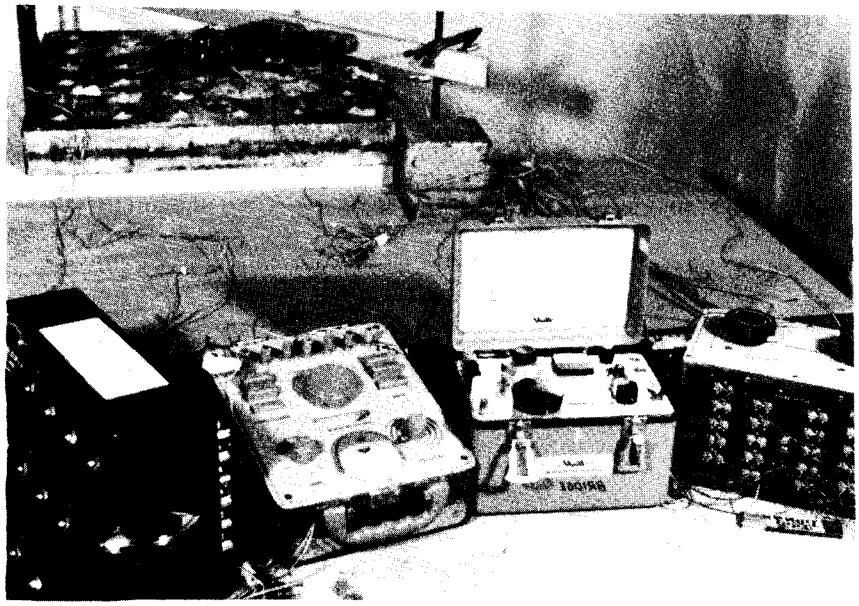

Figure 13. Strain Gage Monitors

In view of the complex factors described, the data obtained from the rosettes showed no pattern which would lend itself to easy interpretation. Indeed, because the effects of fabrication error appear to be as great as the effects of prestressing, further research (beyond the scope of this study) is needed to come to grips with the exact nature of the prestressing problem. It is expected, however, that at larger scale model tests or in full-scale panels, the relative order of magnitude of the fabrication errors would be much less than in the small-scale panels used in this study. (A similar analogy exists between the problem discussed here and local irregularities in a column buckling test. A given amount of crookedness in a small column is far more critical than that same amount in a large column.)

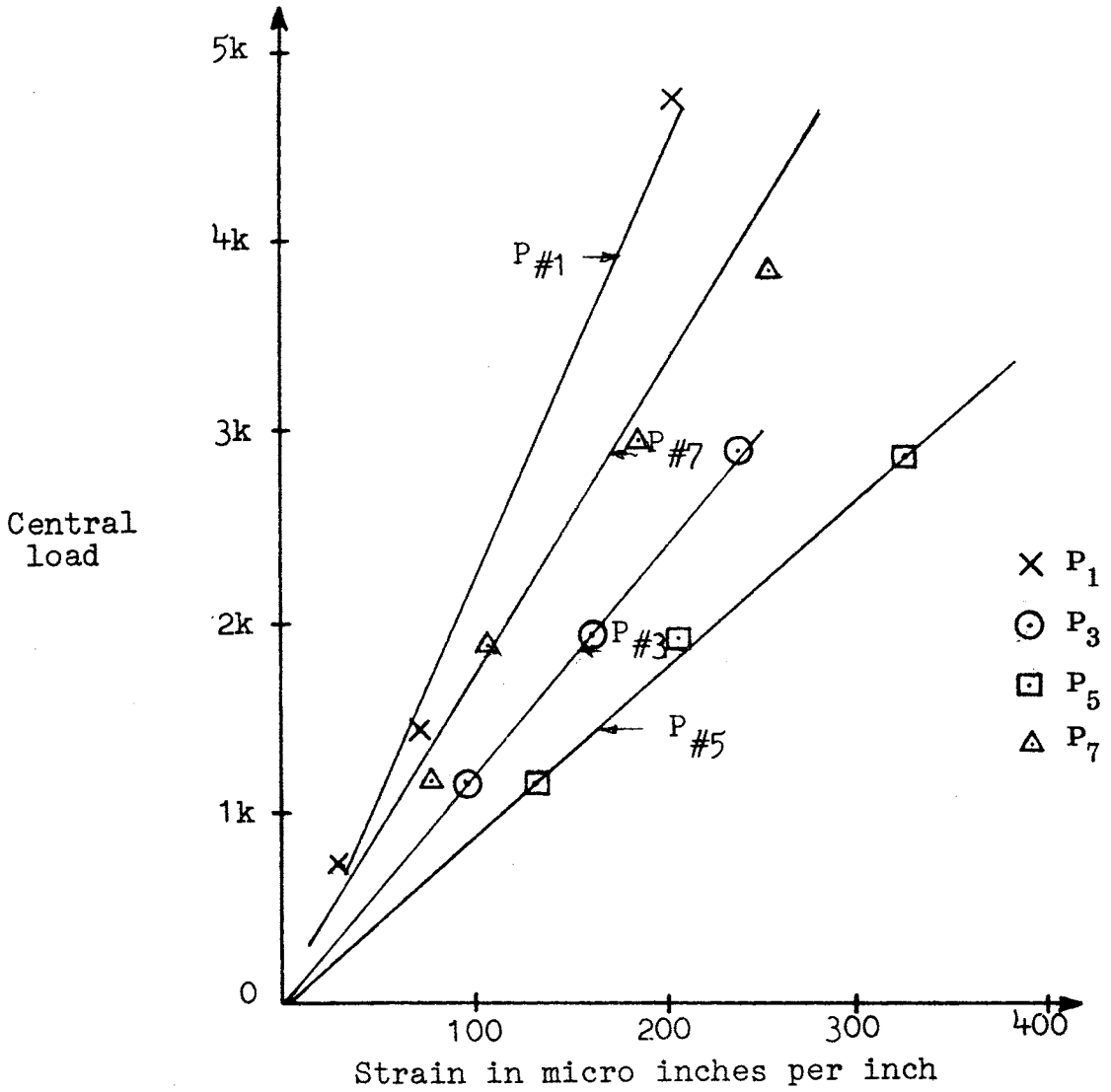

Figure 15. Observed strain readings (strain gage location at center of bottom face plate).

Figure 16 shows the same relationship for a different group of panels, except for a small order reversal between panels P_3, P_7, and P_2 (all of which are very close). Data for panel P_4 are not plotted because of their erratic behavior, attributed to the fact that this panel had only one stud in it. A considerable amount of interface slipping as a result of inadequate horizontal shear resistance probably resulted.

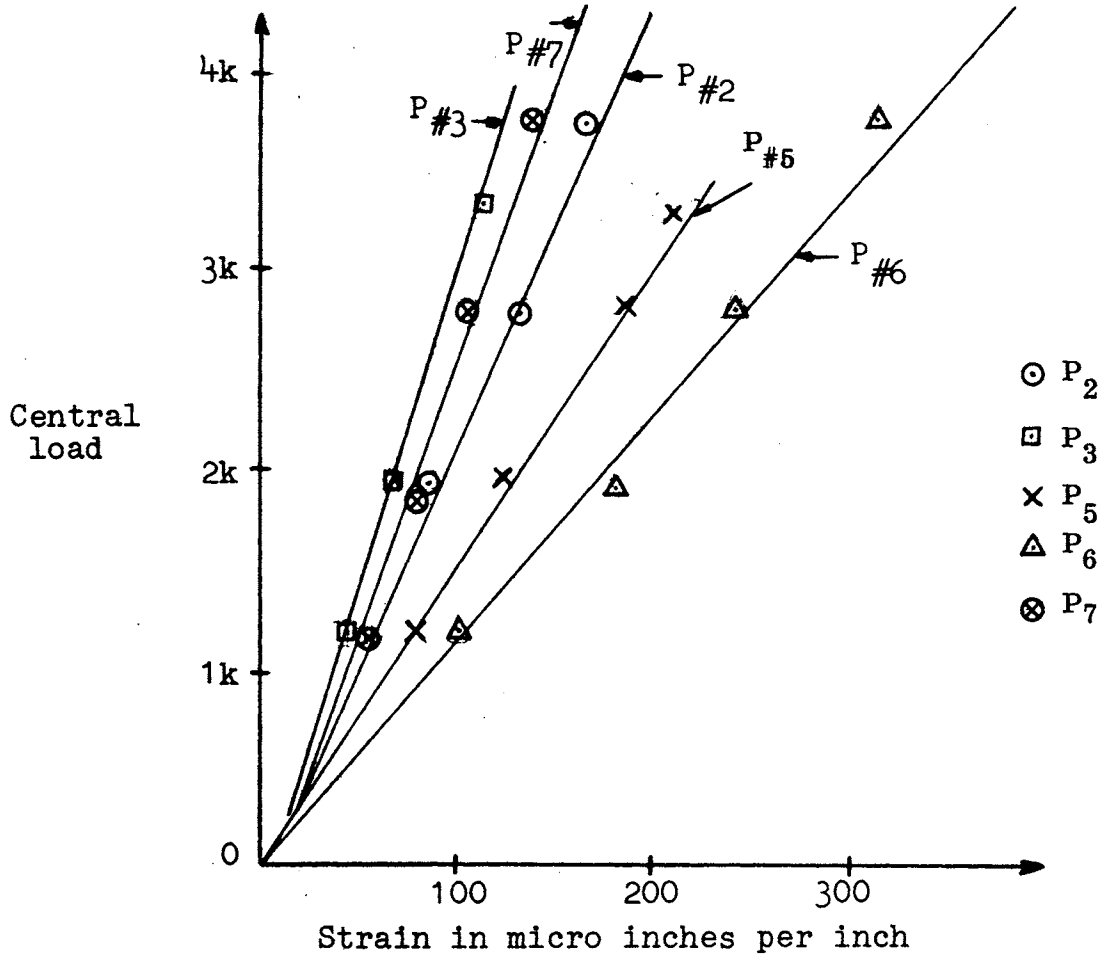

Figure 16. Observed strain readings (strain gage location at bottom face plate, coordinates x, y = 12,8 in inches).

At ultimate load, failure occurred by shear punching near the center of the panel as seen in Figure 17. Figure 18 shows the nature of the diagonal tension failure of the core concrete with the bottom plate removed for examination. Both top and bottom shear plates were deformed but not ruptured at the ultimate load. Shear failure occurred beyond the limit of both the strain gages and the dial gages, which were disconnected or taken off. A plot of ultimate loads, however, is shown in Figure 19.

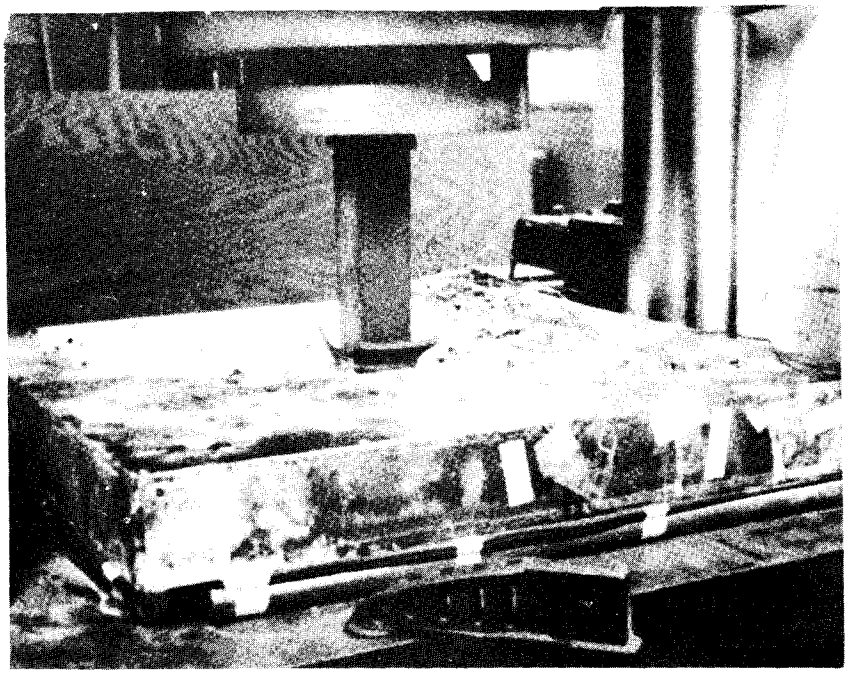

Figure 17. Shear punching of the panel.

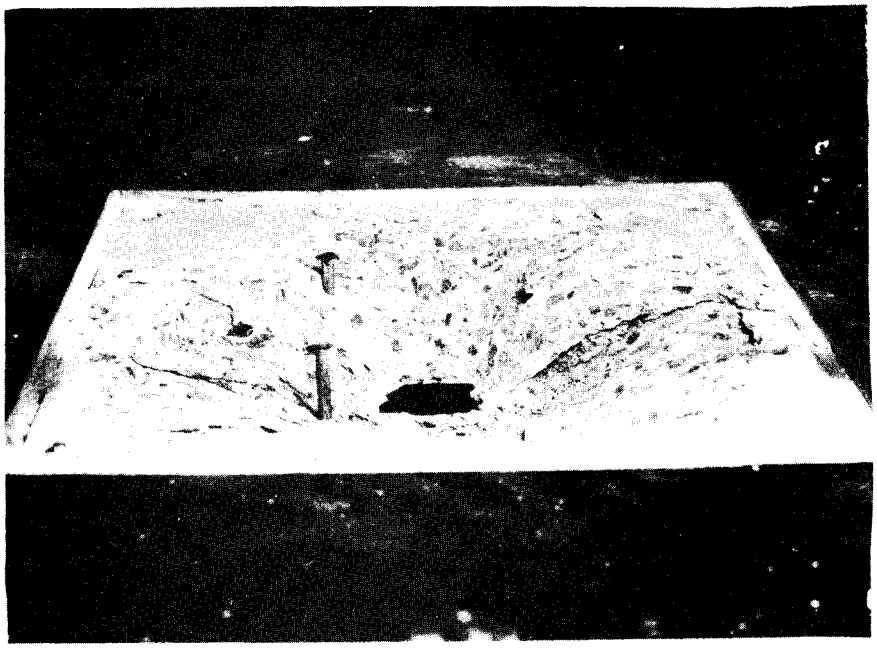

Figure 18. Shear punching failure of the concrete.
(Face plate removed.)

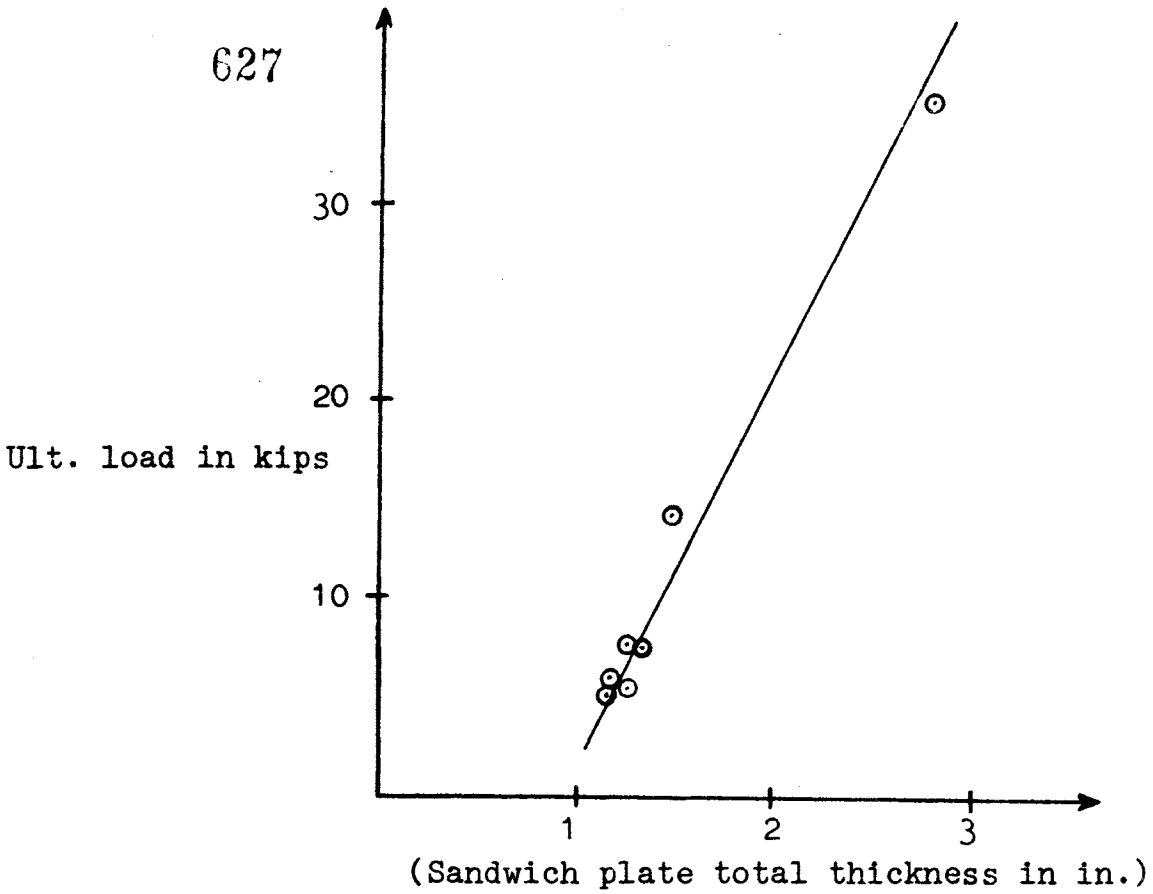

Figure 19. Ultimate concentrated load relation.

Note that at ultimate load, the relationship is linear with the thickness of the panel and independent of the number of studs (as the failure is local).

An emperical relationship of this graph is given by the equation

$$P_u = 5 + 18.2\ (h - 1.15) \qquad \text{--- Eq. (2)}$$

where P_u = ultimate concentrated load in kips

h = total thickness of the panel in inches (assuming it is always greater than 1.15 inches)

The last three panels tested were under a state of uniform load. These tests were conducted as follows. Referring to Figure 20, the test panel was set on an open steel box, which rested on the bed of the testing machine. A high support box had to be used so that dial gages for measuring deflections could be mounted underneath.

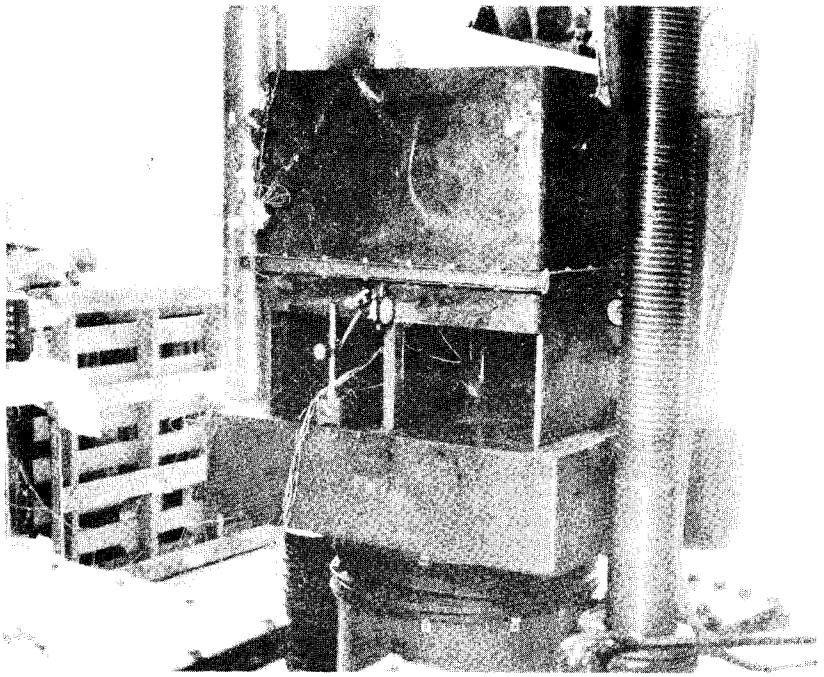

Figure 20. Support frame and sand box assembly for uniform load.

One side of the support box was partially opened for access but it was otherwise solid for rigidity. The top edges of the support box were knife-edged to simulate simple support conditions.

On top of the test panel was placed another four-sided steel box (open at the top and bottom) into which 300 pounds of dry sand were placed. The edges were sealed with neoprene to prevent the escape of sand. Wood planks and steel blocks were placed on the leveled top surface of the sand, onto which the loading head of the testing machine was positioned. The sand thus served to distribute the concentrated load of the machine to a uniform load on to the surface of the panel.

The strain plots for the uniformly loaded panels are shown in Figure 21. As the only known variable in the three plates is the number of studs, it would be expected that panels with more studs would rank above panels with fewer studs. Panel P_{10} with no studs indeed falls below the others, although panel P_9 with 16 studs does rank above P_8 with 36 studs.

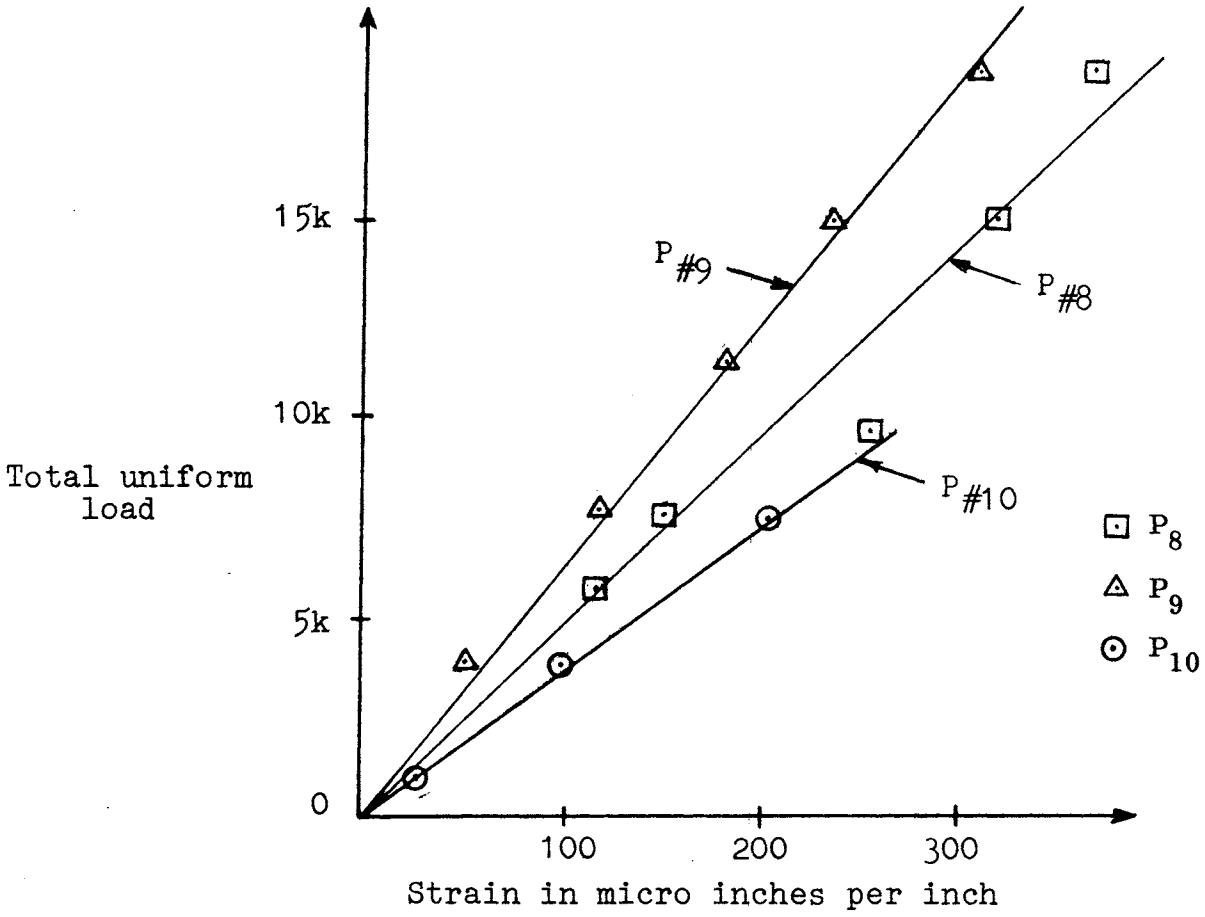

Figure 21. Observed strain readings (strain gage location at center of bottom face plate).

Observing Figure 22, a plot of deflections of the panels (considered to be reliable in this series of tests as the support conditions were less yielding than in the concentrated load tests) it is noted that both panels P9 and P_{10} rank above P_8 in the elastic range. It can only be concluded that in the elastic range of these sandwich panels the number of studs (or the pattern of placement) is not of major importance to strength or deflection. The spread of data is only statistical deviation. Interface shear transfer seems to take place at low stresses primarily by friction between the concrete core and the steel face plate under the pressure of the concrete expansion. As evidenced by the erratic behavior of Panel P_4 (with just one stud), such friction, however, is not a factor to be totally relied upon as it is often accompanied by some slip. The analytical aspects of this problem will be taken up in the next section under Mathematical Analysis.

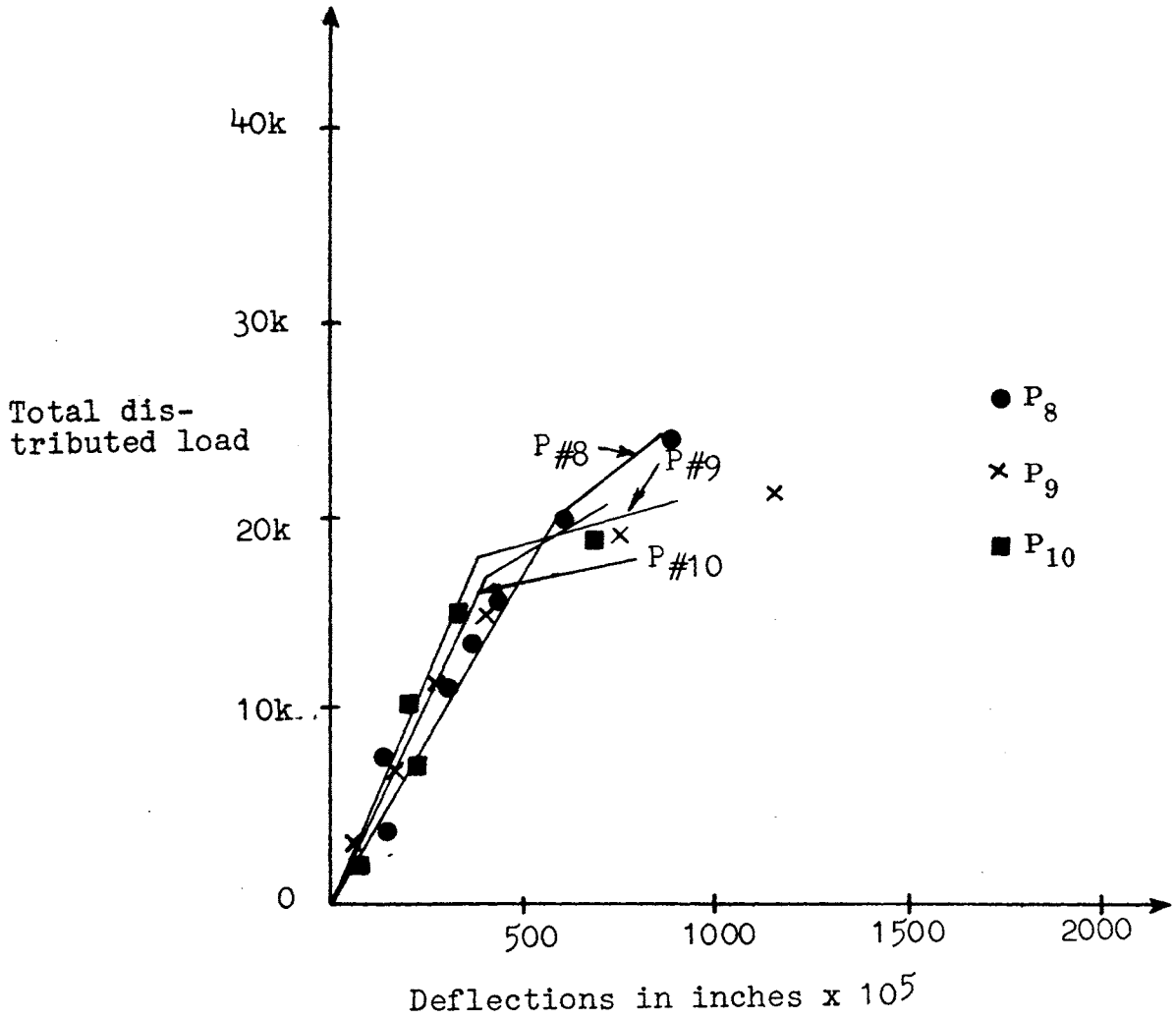

Figure 22. Deflections of center of plate under uniformly distributed load.

At loads beyond elastic behavior, Figure 22 does show that the presence of more studs will affect the ultimate behavior beneficially. As large frictional slip takes place at the interface, the studs take over the shear transfer role. (This condition is analogous to the shear load transfer that takes place between two plates in tension, bolted together. At low loads the shear load is transmitted entirely by friction; but once a large slip takes place at a high load, the bearing action of the bolt enters play.)

It may be noted that ultimate failure loads were not obtained in this series of uniform load tests, although a total load in excess of 144 kips was applied to panel P_8 with no sign of it having reached its limit. Figure 23 shows the nature of the loaded surface after the elastic limit was exceeded. The bending action controls here as opposed to the shear action in the concentrated load tests.

Several final comments, which apply to all the test panels studied, are appropriate. The first is that in the elastic region the strain readings for the upper and lower face plates, when compared, are not considerably different; this finding indicates the existence of the neutral plane at the mid depth of the sandwich panel. It also implies that the concrete core remains uncracked, even in the normal tension region, because of the presence of the chemical prestressing and triaxial restraint.

The second comment, in reference to ultimate strength, is that in these sandwich panels failure always occurs gradually, starting first at the center and then progressing outward. This is evidenced by both visual means and by the noted rate of change of the readings on the dial gages. Rapid dial gage movements always started at the center.

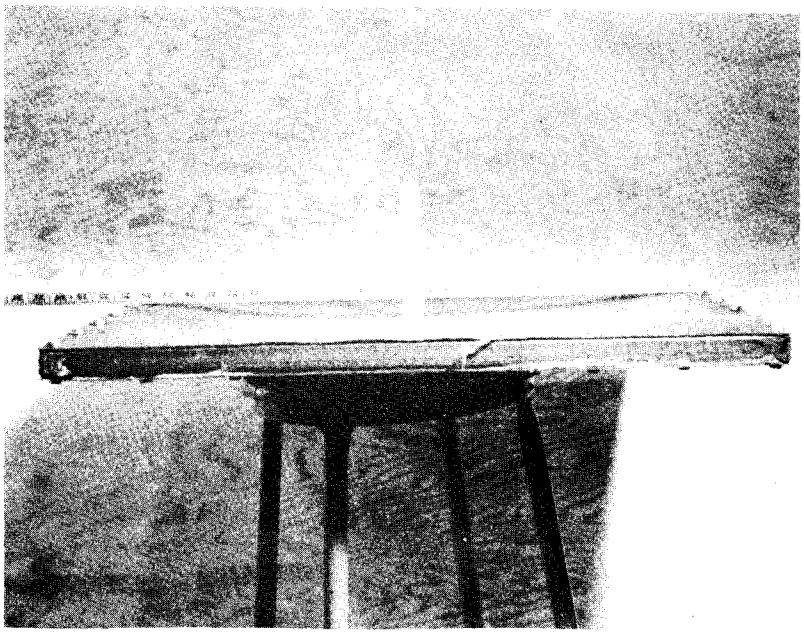

Figure 23. Typical upper face deformation under uniform load.

MATHEMATICAL ANALYSIS

This section of analysis is divided into two parts; the first deals with stresses and deformations associated with the prestressing alone, and the second deals with stresses and deformations associated with the application of the external load.

Further subdividing the behavior of the panel under prestressing, three basic elements are involved; namely the stud, the core, and the face plates. (Side plates could be considered a fourth element, but since knowledge of their exact behavior is not essential to the general understanding of the action of the sandwich panel, they will not be included in this report.)

Referring to Figure 24, an isolated stud is shown acted upon by prestressing forces σ'_z in the Z direction (the direction of the stud axis). In actuality, the expansion pressure σ'_z on the plates varies nonlinearly between studs, being maximum near the stud (where the stud-plate restraint is largest), and minimum at the center point between studs (where expansive restraint is least). As is commonly done in stress analysis, this variable pressure distribution will be replaced with a uniform distribution on a limited effective or equivalent area. As previously discussed, test data on this aspect could not be obtained with the testing procedures used; however, it would be reasonable to assume that

$$F \cong 12\,t \qquad \text{--- Eq. (4)}$$

but not to exceed 0.4 times the distance between studs. This assumption is presented intuitively at this time, until more rigorous analysis can be brought to bear on this aspect of localized stresses. (See pp. 37-38 on further work needed.)

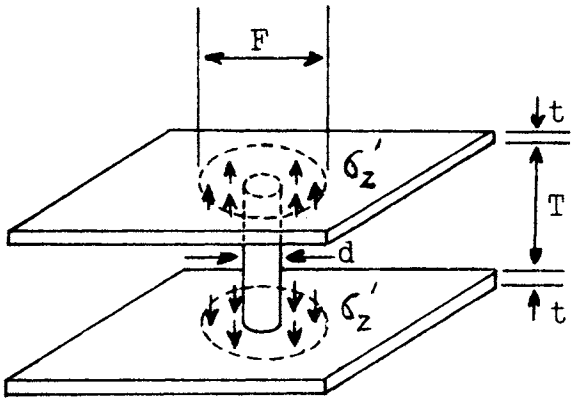

Figure 24. Stud under prestressing.

Thus from equation (1), previously presented, the percentage of tensile elongation in the stud can be found as

$$r = K \ (p + q)^{-m} \qquad \text{--- Eq. (1)}$$

where

$$p = 100 \ \frac{d^2}{F^2}$$

(Other terms are defined in the section on Properties of Core Materials.)

The prestressing stress in the stud is therefore

$$\sigma_s = \frac{r}{100} E_s \qquad \text{--- Eq. (5)}$$

where E_s is the modulus of elasticity for steel. From equilibrium, the compressive stress in the concrete near the stud in the Z direction is approximately

$$\sigma_z' \cong \frac{\sigma_s d^2}{F^2} \qquad \text{--- Eq. (6)}$$

Since the concrete core expands in the X and Y directions as well as in the Z direction, biaxial tensile stresses in the plane of the face plates will develop. (Top and bottom face plates are assumed to be the same thickness.)

The unit strain in the X (or Y) direction of the face plate when under uniform stress ($\sigma_x = \sigma_y$) from basic mechanics is

$$\varepsilon_x = \frac{\sigma_x}{E} \ (1 - \nu) \qquad \text{--- Eq. (7)}$$

where ν is the Poisson's ratio of steel. Thus, combining equation (1) and equation (7), the planar stress in the steel face plate is

$$\sigma_x = \sigma_y = \frac{r E_s}{100(1 - \nu)} \qquad \text{--- Eq. (8)}$$

where p in equation (1) equals $\frac{100\,t}{t + T/2}$

From equilibrium, the compressive prestress stress in the concrete core in the X or Y direction equals

$$\sigma_x' = \sigma_y' = \frac{2\,t\,\sigma_x}{T} \qquad \text{--- Eq. (9)}$$

The bulging of the face plates in the Z direction can be obtained theoretically from a solution of the classical plate equation as found in reference (2), pg. 81.

$$\frac{\partial^4 w}{\partial x^4} + 2\frac{\partial^4 w}{\partial x^2 \partial y^2} + \frac{\partial^4 w}{\partial y^4} = P + N_{xx}\frac{\partial^2 w}{\partial x^2} + N_{yy}\frac{\partial^2 w}{\partial y^2} \quad \text{--- Eq. (10)}$$

where w is the face plate deflection

$N_{xx} = N_{yy} = \sigma_x t = \sigma_y t$ (as found from Eq. (8))

$P = \sigma_z'$ (within distance F/2 of stud) and assumed zero elsewhere

If only bending displacements are required, the deflection "w" at the stud may be assumed equal to zero. Otherwise, the displacement caused by the elongation of the stud must be added to "w". The solution of equation (10) by the numerical method of finite differences (assisted by a digital computer) is recommended. See reference (3).

Consider next the mathematical analysis of the sandwich plate under an external load. Only the behavior below the elastic limit of the materials will be considered. Because of the complex nature of the analysis, numerous mathematical strategies and assumptions were explored. Presented in this report, however, is only the one that appears to be consistent with the observed behavior in all important respects. First, it is assumed that at low (working) loads shear transfer between the face plates and the core is through friction, rather than through the studs. (Tests indicate that this friction is elastically reversible at low loads.) This assumption is consistent with the findings of studies of composite beams of steel and concrete joined by stud connections, (ref. 3 and 4). Secondly, it is assumed that a certain amount of interface slip may take place simultaneously in the upper and lower interfaces. The slip is assumed to be proportional to the first partial derivative of the vertical panel displacement "w" with respect to x or y as given by the parameter s.

$$s_x = -k\,w_{,x} \quad \text{and} \quad s_y = -k\,w_{,y} \quad \text{--- Eq. (11)*}$$

where k is an empirical slip factor ranging from 0 to 0.5.

See Figure 25 for a diagram of the assumed cross-sectional displacement, showing the slip. The parameters U and V are displacements of points in the panel in the X and Y directions respectively.

---

*Partial derivatives are shown by the comma notation rather than by the fractional notation.

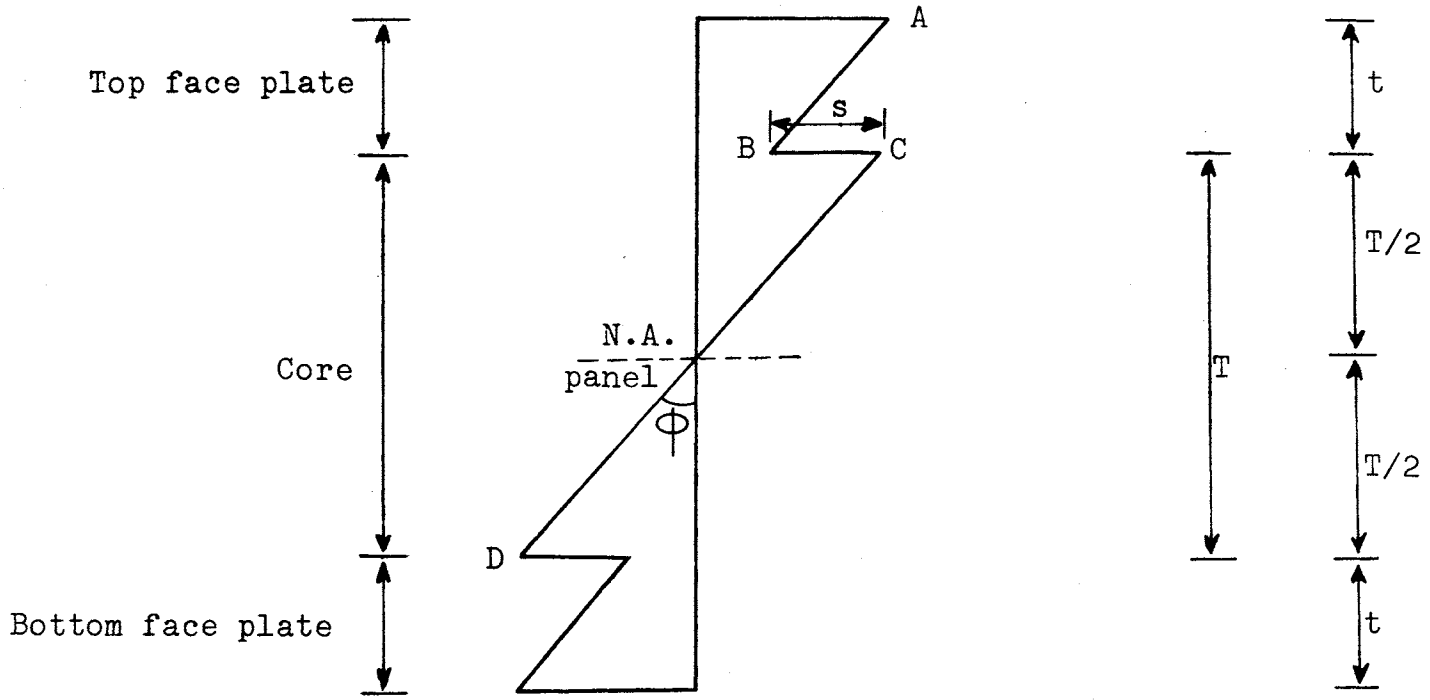

Figure 25. Displacement diagram.

The general expression for the strains are

$$\varepsilon_{xx} = U_{,x} = (z\,\phi_x)_{,x}$$

and $$\varepsilon_{yy} = V_{,y} = (z\,\phi_y)_{,y}$$

which for the outermost fibre of the upper face plate becomes

$$\varepsilon_{xt} = (T/2 + t)\,\phi_{x,x} - s_{x,x}$$

because $$U = (T/2 + t)\,\phi_x - s_x$$

The strain at the top interface is $\varepsilon_{x\,i\,t} = (T/2)\,\phi_{x,x} - S_{x,x}$

because segment $AB \parallel CD$

The average strain in the upper face plate $= (1/2)(\gamma_{x\,t} + \gamma_{x\,i\,t})$

Thus for the upper face plate

$$\varepsilon_{x_{av.}} = (T/2 + t/2)\,\phi_{x,x} - S_{x,x}$$ in the X direction

and in the same way

$$\varepsilon_{y_{av.}} = (T/2 + t/2)\,\phi_{y,y} - S_{y,y}$$ in the Y direction

The strains in the core, at a distance of T/2, are

$$\varepsilon_{x\,T/2} = (T/2)\,\phi_{x,x} \quad \text{and} \quad \gamma_{y\,T/2} = (T/2)\,\phi_{y,y}$$

and

$$\varepsilon_{x\,o} = \varepsilon_{y\,o} = 0$$ at the neutral plane.

Because of symmetry, the magnitude of the strains in the bottom half of the panel are the same as that in the top half.

From standard plate theory (ref. 2) the following basic relations of compatibility and equilibrium can also be stated.

$$\sigma_x = \frac{E}{1-\nu^2}\left(\varepsilon_{x\,x} + \nu\,\varepsilon_{y\,y}\right)$$

$$\sigma_y = \frac{E}{1-\nu^2}\left(\varepsilon_{y\,y} + \nu\,\varepsilon_{x\,x}\right)$$

M_x = (bending in X direction per unit length) $= \int \sigma_x\, z\, dz$

M_y = (bending in Y direction per unit length) $= \int \sigma_y\, z\, dz$

Thus, by substitution,

$$M_x = \frac{E_s}{1-\nu_s^2}\left[(T/2 + t/2)(\phi_{x,x} + \nu_s \phi_{y,y}) - (s_{x,x} + \nu_s s_{y,y})\right]$$

$$t(T+t) + \frac{E_c}{1-\nu_c^2}(\phi_{x,x} + \nu_c \phi_{y,y})\frac{T^3}{12} \qquad \text{--- Eq. (12)}$$

$$M_y = \frac{E_s}{1-\nu_s^2}\left[(T/2 + t/2)(\phi_{y,y} + \nu_s \phi_{x,x}) - (s_{y,y} + \nu_s s_{x,x})\right]$$

$$t(T+t) + \frac{E_c}{1-\nu_c^2}(\phi_{y,y} + \nu_c \phi_{x,x})\frac{T^3}{12} \qquad \text{--- Eq. (13)}$$

From basic elasticity

$$\varepsilon_{xy} = U_{,y} + V_{,x}$$

$$= z(\phi_{x,y} + \phi_{y,x})$$

τ_{xy} = (shear per unit length) = $\int G\, \varepsilon_{xy}\, dz$

where G is the shear modulus (the subscript s denotes steel and the subscript c denotes concrete)

M_{xy} = (twist per unit length) = $\int \tau_{xy}\, z\, dz$

By substituting the displacement relationships,

$$M_{xy} = G_s\left[(T/2 + t/2)(\phi_{x,y} + \phi_{y,x}) - (s_{x,y} + s_{y,x})\right]$$

$$t(T+t) + G_c(\phi_{x,y} + \phi_{y,x})\frac{T^3}{12} \qquad \text{--- Eq. (14)}$$

Again from standard plate theory (ref. 2)

$$M_x = -D\left(w_{,xx} - \nu w_{,yy}\right)$$

$$M_y = -D\left(w_{,yy} - \nu w_{,xx}\right)$$

$$M_{xy} = D\left(1-\nu\right) w_{,xy}$$

$$M_{x,xx} + M_{y,yy} - 2\,M_{xy,xy} + P = 0 \qquad \text{--- Eq. (15)}$$

where D = stiffness modulus of panel

P = normal load per unit surface

Assuming $s_x = s_y$

and substituting into equation (15), the basic differential equation for the externally loaded sandwich panel with slip becomes

$$\left\{ \frac{E_s}{1-\nu_s^2}\left[t/2\,(T+t)(T+t-kT)\right] + \frac{E_c}{1-\nu_c^2}\left(T^3/12\right)\right\} \nabla^4 w = P$$

--- Eq. (16)

where $$\nabla^4 w = \frac{\partial^4 w}{\partial x^4} + 2\,\frac{\partial^4 w}{\partial^2 x\,\partial^2 y} + \frac{\partial^4 w}{\partial y^4}$$

Because the concrete core is relatively stiff, shear terms are not necessary as in normal sandwich plate theory. The entire term inside the { } in equation (16) becomes the effective stiffness modulus "D" for the panel.

Equation (16) is best solved numerically by any standard finite difference method with the aid of a digital computer (see ref. 5). Equation (16) was in this manner solved for panels P_8 through P_{10} assuming a uniform load P = 29 psi for various values of k ranging from zero to 0.5. Figure 26 shows the influence of the slip on the deflection of the panels.

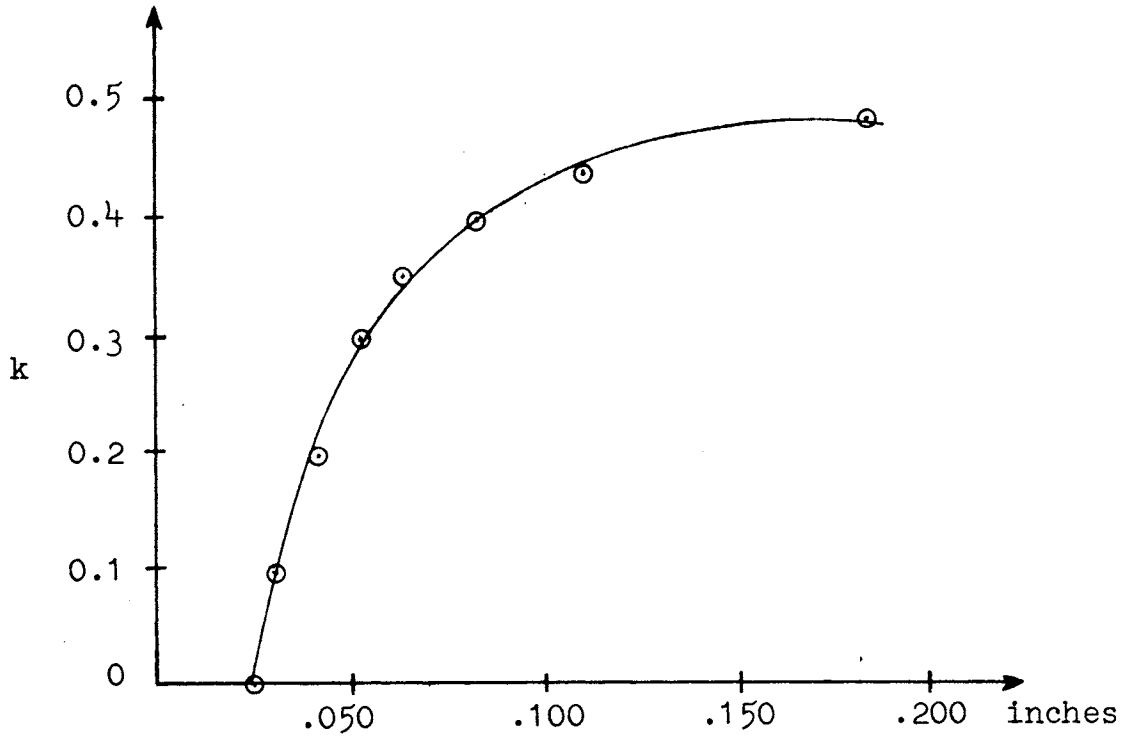

Figure 26. Central deflection with various amounts of slip.

Once the deflections "w" are determined for any given situation, the other equations presented in this section may be applied, point by point, to solve for the flexural stresses in the steel and concrete at any location. For the type of panels tested, the maximum stresses and deflections occur at the center of the panel.

CONCLUSIONS

Using panel P_8 as an example, a mathematical analysis was made according to the theory described. Figure 27 shows the excellent agreement between the experimental test results and the mathematical theory. Table 5 further shows for this same panel the comparison of stresses. Note that a slip factor "k" of 0.25 correlated well with both deflection and stress data. (Prestress stresses are taken into account in Table 5.)

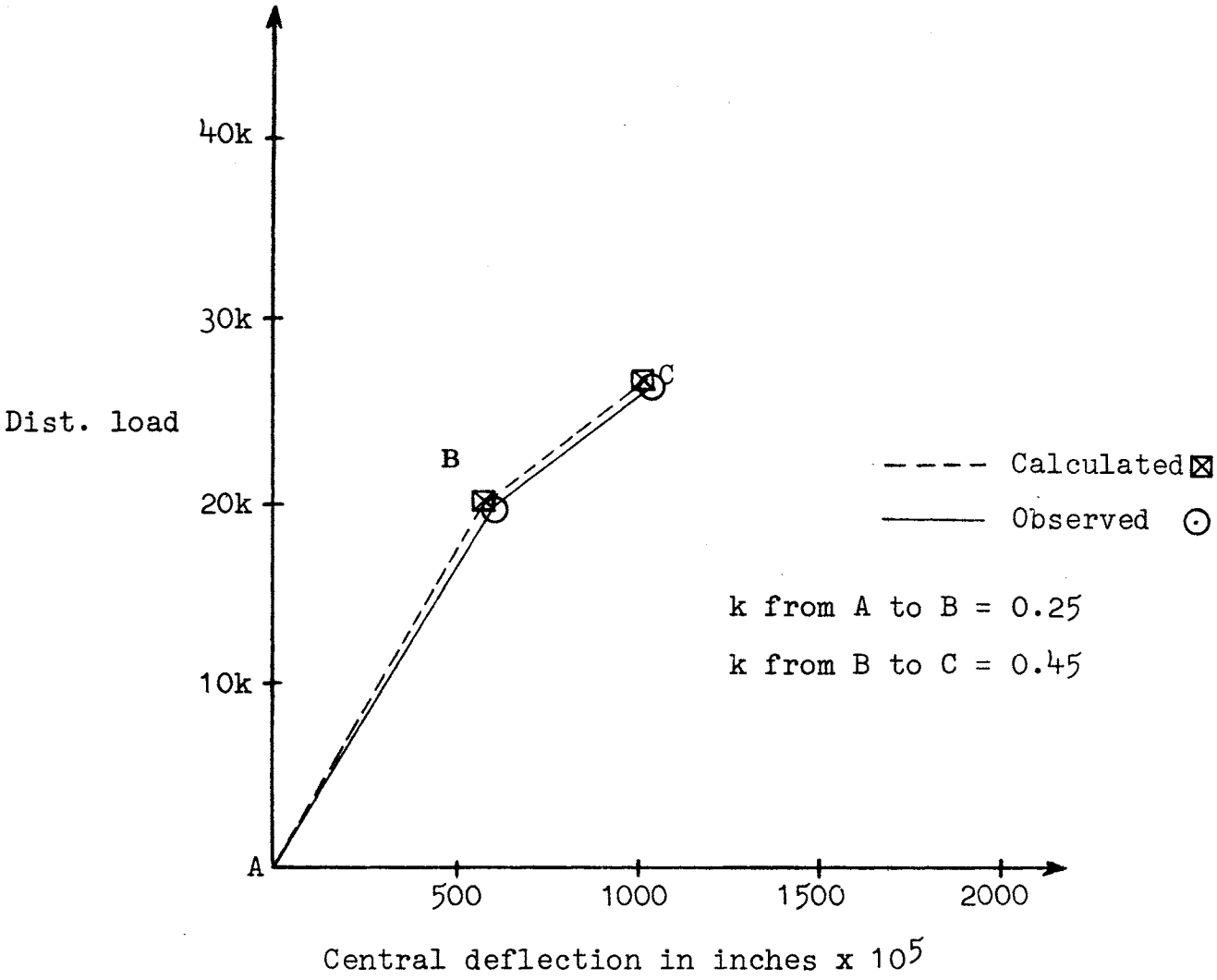

Figure 27. Deflection comparison of experiment and theory (Panel P_8).

TABLE 5

STRESS COMPARISON OF EXPERIMENT AND THEORY (PANEL P_8)

Load (psf)		Observed	Analytical	
			k = 0	k = .25
		4200 psf	4200 psf	4200 psf
Central Deflection	inches	0.046	0.025	0.044
	Δ/L L = span	1/510	1/1020	1/535
Stress in Steel (psi)	Top fibre	3400	400 (t)	3050 (c)
	Bot. fibre	21000	19100 (t)	22440 (t)
Stress in Concrete (psi)	upper intf.	Not obs.	406 (c)	537 (L)
	lower inf.	Not obs.	32 (c)	99 (t)

c = compressive stress
t = tensile stress

For additional comparison, stress and control deflection values are given in Table 5 for a theoretical no slip condition of k = 0. Particularly large reductions are to be noted in the latter case in deflections, although the magnitudes of the maximum stresses are not greatly changed. (Similar conclusions were reached after an analysis of plate P_3, loaded with a concentrated force.)

It may also be deduced from Table 5 that at point B in Figure 27, where a rate increase in deflection begins to occur, the maximum steel stress (26,000 psi) begins to approach its yield stress (33,000 psi). This factor probably triggers the increase of large interface slipping.

The general consistency of the experimental data and the mathematical analysis seems to indicate that the proposed theory is valid.

Still another comparison of practical importance is shown in Table 6. Here, two panels, identical with regard to the amount of concrete and the amount of steel, are studied. Both are 5.45 inches thick and both reinforced with 2.750% of steel.

TABLE 6

COMPARISON OF STANDARD R. C. SLAB AND SANDWICH PANEL
(Based on Calculated Results)

		R. C. Slab	Sandwich Panel
Thickness (inches)		5.45	5.45
Reinf. (%)		2.75	2.75
Maximum ext. load stress (ksi)	Steel	18.0	17.78
	Conc.	1.24	0.39
Maximum prestr. stress (ksi)	Steel	—	0.22
	Conc.	—	0.22
Maximum total stress (ksi)	Steel	18.0	18.0
	Conc.	1.24	0.89
Load (ksf)		33.0	46.5
Defl. (inches)		0.0132	0.0101

Both are simply supported square panels spanning 23.5 inches in each direction. However, one is a standard reinforced concrete slab, reinforced with standard steel bars, while the other is a sandwich panel of the type discussed in this report. At the working limit of the standard R. C. panel, its allowable uniformly distributed load is computed to be 33.0 kips per square foot. For the same stress limit, the sandwich panel is able to carry a load of 46.5 kips per square foot, or a load 41% greater. Yet, the deflection at this greater load is almost 23% less than that for the standard R. C. panel. The conclusion is that sandwich panels are both stronger and stiffer than normal R. C. slabs using the same amount of steel and concrete.

It is the opinion of the authors that this favorable comparison justifies continued research and development of sandwich panels for bridge decks (as well as other structural uses where high strength to weight ratios are needed). The laboratory tests further proved that such sandwich panels possess great strength reserves beyond the elastic range in the event of overload.

FURTHER WORK

Under conditions of limited manpower, time and funds, an assortment of detailed studies and problems had to be bypassed in this study to establish the general feasibility of sandwich panels as proposed. Most of these problems were mentioned in the main body of this report; however, the areas in which further research is indicated are summarized here.

1. Expanding concrete characteristics under biaxial and triaxial restraint.
2. Expansion characteristics of the panel through its thickness.
3. Stresses in the face plate, stud, and concrete in the region of the stud.
4. Stresses in the region of the side plates.
5. Micro behavior of the interface slip.
6. Criteria for stud size and spacing.
7. Prediction of ultimate strength behavior (flexure and shear).
8. Dynamic and fatigue behavior of the panels.
9. Tests of full-scale panels (to eliminate small-scale model errors) in the laboratory and in the field.
10. A simple design procedure.
11. The most economical method of fabrication, including corrosion protection and skidproofing.

The work yet needed to make the proposed sandwich panel practical for bridge construction is admittedly considerable. However, the potential for developing a much stronger, lighter, and possibly less expensive bridge is believed to have been demonstrated by this study.

ACKNOWLEDGEMENTS

644

The authors thank all those staff technicians who assisted with the testing program (often in the face of considerable obstacles); professors in the Department of Civil Engineering at the University of Virginia for their advice and cooperation; the administrators in the Virginia Highway Research Council and Federal Highway Administration for their financial support and encouragement; and, finally, the clerical staff and Report Section of the Virginia Highway Research Council for preparing this final report.

REFERENCES

1. Journal of the American Concrete Association, "Expansive Cement Concrete-Present State of Knowledge," paper #67-35, August 1970. (Contains 62 additional references on the subject.)

2. S. Timoshenko and S. Woinowsky-Krieger, Theory of Plates and Shells, McGraw-Hill Book Company, 1959.

3. C. P. Siess, I. M. Viest and N. M. Newmark, "Studies of Slab and Beam Highway Bridges: Part III, Small-Scale Tests of Shear Connectors and Composite T-Beams," University of Illinois Engineering Experimental Station, Bulletin Series No. 396, February 1952.

4. N. M. Hawkins, "The Influence of the Properties of the Stud on the Behavior of Composite Beams," Department of Civil Engineering Report, University of Washington, Seattle, May 1971.

5. P. C. Wang, Numerical and Matrix Methods in Structural Mechanics, Wiley & Sons, 1966.

6. F. J. Plantena, Sandwich Construction, Wiley & Sons, 1966.

7. H. G. Allen, Analysis and Design of Structural Sandwich Panels, Pergamon Press, 1969.